The UV-A Receptor CRY-DASH1 Up- and Downregulates Proteins Involved in Different Plastidial Pathways

Anxhela Rredhi, Jan Petersen, Volker Wagner, Trang Vuong, Wenshuang Li [†] Wei Li, Laura Schrader and Maria Mittag [*]

Matthias Schleiden Institute of Genetics, *Bioinformatics and Molecular Botany, Friedrich Schiller University Jena, 07743 Jena, Germany*

Correspondence to Maria Mittag: *M.Mittag@uni-jena.de (M. Mittag) @1anPetersen (J. Petersen), @trangha593 (T. Vuong)*
https://doi.org/10.1016/j.jmb.2023.168271
Edited by Volha Chukhutsina

Abstract

Algae encode up to five different types of cryptochrome photoreceptors. So far, relatively little is known about the biological functions of the DASH (*Drosophila, Arabidopsis, Synechocystis* and *Homo*)-type cryptochromes. The green alga *Chlamydomonas reinhardtii* encodes two of them. CRY-DASH1 also called DCRY1 has its maximal absorption peak in the UV-A range. It is localized in the chloroplast and plays an important role in balancing the photosynthetic machinery. Here, we performed a comparative analysis of chloroplast proteins from wild type and a knockout mutant of *CRY-DASH1* named *cry-dash1*$_{mut}$, using label-free quantitative proteomics as well as immunoblotting. Our results show upregulation of enzymes involved in specific pathways in the mutant including key enzymes of chlorophyll and carotenoid biosynthesis consistent with increased levels of photosynthetic pigments in *cry-dash1*$_{mut}$. There is also an increase in certain redox as well as photosystem I and II proteins, including D1. Strikingly, CRY-DASH1 is coregulated in a D1 deletion mutant, where its amount is increased. In contrast, key proteins of the central carbon metabolism, including glycolysis/gluconeogenesis, dark fermentation and the oxidative pentose phosphate pathway are downregulated in *cry-dash1*$_{mut}$. Similarly, enzymes of histidine biosynthesis are downregulated in *cry-dash1*$_{mut}$ leading to a reduction in the amount of free histidine. Yet, transcripts encoding for several of these proteins are at a similar level in the wild type and *cry-dash1*$_{mut}$ or even opposite. We show that CRY-DASH1 can bind to RNA, taking the *psbA* RNA encoding D1 as target. These data suggest that CRY-DASH1 regulates plastidial metabolic pathways at the post-transcriptional level.

Introduction

Cryptochromes are flavin-binding photoreceptors that can be found in bacteria, fungi, algae and land plants as well as in animals.[1–3] They mainly absorb in the UV-A and blue light range but can also absorb red light depending on the redox state of the flavin.[4,5] Although they evolutionary derived from the DNA-repair enzyme class of photolyases, only some cryptochromes still possess DNA-repair function.[6,7] Cryptochromes were first described in the plant *Arabidopsis thaliana* where they regulate development and plant growth.[8] They are also involved in the circadian clock, functioning either as light sensors of the input pathway such as in *A. thaliana* or being a member of the endogenous oscillator as in mammals.[9,10] Moreover, cryptochromes are involved in magnetosensing as for example in *A. thaliana* and migrating birds.[11,12]

Photosynthetic protists, named microalgae, are major contributors to global CO_2 fixation, stand at the base of many food webs and influence biogeochemical processes.[13–15] Microalgae use light as a source of energy and information. They have a broad variety of photoreceptors including cryptochromes with different properties and functions.[16,17] In the green model alga *Chlamydomonas reinhardtii*,[18,19] four cryptochromes are encoded in the genome: (i) a plant cryptochrome (pCRY) that is degraded by light, is part of the circadian clock machinery and is involved in controlling the sexual cycle,[20,21] (ii) an animal-like cryptochrome (aCRY) that also controls the sexual cycle, regulates blue- and red-light dependent gene expression and has photolyase activity[4,7,22] and (iii) two *Drosophila*, *Arabidopsis*, *Synechocystis* and *Homo* (DASH)-type cryptochromes,[23] CRY-DASH1 and CRY-DASH2,[24] recently also named DCRY1 and DCRY2.[19]

The CRY-DASH subfamily of cryptochromes is found from bacteria to vertebrates.[25] Some CRY-DASH proteins have DNA-repair activity[26–28] but CRY-DASHs can be also involved in light-regulated development of fungi and macroalgae.[29,30] In *C. reinhardtii*, the function of CRY-DASH1 has been studied recently.[31] CRY-DASH1 is encoded in the nucleus and localized in the chloroplast; it has its absorption peak in the UV-A area.[31] UV-A based growth promotion of the algal cells was found in the wild type but is missing in a *CRY-DASH1* knockout mutant called *cry-dash1*$_{mut}$.[31] Also in the mutant, a reduced growth phenotype was observed compared to the wild type. Yet the mutant is greener as wild type as it has an increased content of the photosynthetic pigments including chlorophylls and carotenoids.[31] In *cry-dash1*$_{mut}$, the chloroplast architecture is altered showing hyper-staking of thylakoid membranes. Some key proteins of photosystem II (PSII) namely D1 and its antenna protein CP43 are upregulated in the mutant while certain light harvesting proteins remain unchanged in their abundance. Taken together, these data led to the hypothesis that CRY-DASH1 balances the photosynthetic machinery by acting as a negative regulator.[31]

Here, we corroborate that the reduced growth of *cry-dash1*$_{mut}$ is due to shielding effects of the mutant cells towards light. Moreover, we discovered that D1 and CRY-DASH1 are coregulated. We performed comparative label-free proteomics of chloroplast proteins from wild type and *cry-dash1*$_{mut}$ cells to investigate the variety of chloroplast proteins that are regulated by CRY-DASH1. While several key enzymes of the chlorophyll and carotenoid biosynthesis as well as some photosystem proteins were upregulated in *cry-dash1*$_{mut}$, enzymes of the central carbon metabolism as well as of histidine biosynthesis were significantly downregulated resulting in decreased levels of free histidine in the mutant. All so far examined transcripts encoding the up- and downregulated proteins, respectively, are not altered in the wild type compared to the mutant or even oppositely regulated. We also found that CRY-DASH1 can bind to a selected mRNA. Taken together, our data suggest that CRY-DASH1 functions as posttranscriptional regulator.

Results and Discussion

Isolation and quantification of chloroplast proteins from wild type and cry-dash1$_{mut}$

The knockout mutant, *cry-dash1*$_{mut}$ lacks CRY-DASH1 protein as verified in immunoblots (Supplementary Figure 1(A), left part[31]). Here, we performed a label-free quantitative comparison of chloroplast proteins from wild type SAG73.72 and *cry-dash1*$_{mut}$. For this purpose, we have grown the cells photoautrophically in minimal medium lacking acetate as carbon source (see Methods). Subcellular chloroplast fractions of both strains were isolated following a published protocol[32] that was adapted to the cell wall containing wild type and mutant strain[31] (see also Methods). We collected the layer with intact chloroplasts at the 45–65% interface of a Percoll gradient (Supplementary Figure 1(B)) for further analysis. The presence of CRY-DASH1 in the wild-type chloroplast fraction was confirmed by immunoblotting (Supplementary Figure 1(A), right part).

For quantitative comparison of the identified proteins from the wild type and the mutant, we had to determine the protein amount from both fractions. For this purpose, the chlorophyll concentration is often used as a standard for protein determination of plastidial proteins.[32,33] However, in our study it was not a viable option because *cry-dash1*$_{mut}$ has higher levels of chlorophylls as mentioned before.[31] This makes chlorophyll concentration unreliable as a marker for determining the concentration of proteins. Due to the presence of bovine serum albumin (BSA) in the chloroplast isolation buffer, traditional methods for measuring protein concentration were also not reliable in this experiment. As an alternative method for determining the protein concentration, we thus chose to quantify the abundance of the large subunit of RuBisCO (rbcL) by immunoblotting. We found that rbcL is similar abundant in its amount in both the wild-type and *cry-dash1*$_{mut}$ lines when comparing its content in total protein extracts (Supplementary Figure 1(C)). After quantification (Supplementary Figure 1(D)), an amount equivalent to 75 μg of isolated chloroplast proteins from wild type and *cry-dash1*$_{mut}$ were separated in a 10% SDS-polyacrylamide-piperazine diacrylamide gel that was sliced into 12 pieces per lane (Supplementary Figure 1(E)). Proteins from each piece were in-gel digested using trypsin. Liquid chromatography electrospray ionization tandem mass spectrometry (LC-ESI-MS/MS) analysis was performed as outlined in

Methods. We performed two independent biological replicates. All identified proteins of the two wild type and mutant replicates, along with the number of their unique peptides are shown in Supplementary Tables 1 and 2 (wild type) and Supplementary Tables 3 and 4 (mutant), respectively.

We identified 1325 proteins that were present in both replicates with at least two different peptides of either wild type or mutant. For further analysis, we focused on the 643 proteins from this list that were annotated (https://phytozomenext.jgi.doe.gov/info/CreinhardtiiCC_4532_v6_1) as chloroplast proteins (Supplementary Tables 1–4 (chapter A)); the others were considered as contaminants (Supplementary Tables 1–4(chapter B)). It should be mentioned that chloroplast encoded genes are recognizable by their ID number that starts with "CreCp" in Supplementary Tables 1–4(chapter A) in contrast to nuclear encoded chloroplast proteins that start with "Crexx" whereby xx represent numbers. This also holds true for Tables 1 and 2.

For quantitative comparison, we applied the label-free quantitative normalized spectral abundance factor (NSAF) procedure, which provides a reliable estimation of the relative protein abundance without the use of isotopic labeling. A NSAF threshold of $\geq$1.33 was used to identify upregulated proteins, whereas a threshold of $\leq$0.75 was used to identify the downregulated proteins.[34,35] Of the 643 chloroplast proteins, 121 proteins showed differential expression levels in the *cry-dash1*$_{mut}$ strain compared to wild type (Tables 1 and 2). Hereby, 61 plastidial proteins were downregulated in the mutant (Table 1), and 60 plastidial proteins were upregulated (Table 2). In some cases, we detected a given plastidial protein only in the mutant or in the wild type. These proteins are also included in Tables 1 and 2.

CRY-DASH1 acts as a positive regulator on the central carbon metabolism and the histidine biosynthesis

Strikingly, CRY-DASH1 acts not only as negative regulator as we showed previously[31] (see also next chapter), causing upregulation of certain pathways when it is missing. Here, we found that CRY-DASH1 can also act as an activator and thus its absence also causes downregulation of some pathways (Table 1). The major affected pathway is the central carbon metabolism,[36,37] including the part of glycolysis compartmentalized to the chloroplast in *C. reinhardtii* (from hexose-phosphate to 3-phosphoglycerate), gluconeogenesis, the pentose phosphate pathway and the dark fermentative metabolism. Several enzymes of the first two mentioned pathways are downregulated in *cry-dash1*$_{mut}$ (Table 1 and Figure 1(A)) like phosphoglucomutase 1 (PGM1), phosphofructokinase (PFK1), glycerol-3-phosphate dehydrogenase (GPD4), glyceraldehyde 3-phosphate dehydrogenase (GAPC1) or fructose1,6-bisphosphate aldolase (FBA2). Enzymes involved in the pentose phosphate pathway such as transaldolase (TAL1) and 6-phosphogluconate dehydrogenase (GND1) are also downregulated in *cry-dash1*$_{mut}$ as well as key enzymes playing a role in dark fermentation of *C. reinhardtii.* The latter include pyruvate kinase (PYK1), pyruvate-formate lyase (PFL1) and phosphate acetyltransferase (PAT2) (Table 1 and Figure 1(A)).

In its natural habitat as a soil alga, *C. reinhardtii* spends significant parts of its life cycle under light-limiting and hypoxic/anoxic conditions, especially in the evening. Under these conditions, the fermentative metabolism is activated.[37,38] During anoxia generated acetyl-CoA may be metabolized to acetate catalyzed by PAT2 (Figure 1(A)). We positively confirmed the decrease of the PAT2 protein by performing immunoblots using commercially available antibodies against PAT2 (Figure 1(B)). Also, the acetyl-CoA synthetase/ligase (ACS3) that is involved in acetate assimilation is downregulated in the mutant. This data highlights that a cryptochrome photoreceptor has an important regulatory role as a positive regulator of the central carbon metabolism of *C. reinhardtii*.

In contrast to the proteins, the transcript levels of cytoplasmic *PAT2, PYK1* and *PFL1* did not show a significant difference in wild type and *cry-dash1*$_{mut}$ (Figure 1(C)). Thus, CRY-DASH1 appears to act at the posttranscriptional, presumable translational level, at least in these three cases.

Certain components, such as enzymes involved in amino acid biosynthesis seem to be differentially regulated (Tables 1 and 2), depending on the type of amino acid. Here, we focused on histidine biosynthesis that seems downregulated in the mutant based on the decreased levels of the involved enzymes N-5-phosphoribosyl-ATP transferase (HIS1) and imidazole glycerol phosphate synthase (HIS7) (Table 1, Figure 1(D)). We analyzed whether this regulation is reflected by the amount of free histidine. Indeed, the amount of free histidine is significantly reduced in *cry-dash1*$_{mut}$ compared to the wild type (Figure 1(E)). We also verified whether this reduction in free histidine in *cry-dash1*$_{mut}$ can be complemented using a priorly established complementing line[31] abbreviated as compl$_{38}$ that expresses CRY-DASH up to 53%. In compl$_{38}$, free histidine is significantly enhanced compared to *cry-dash1*$_{mut}$ while there is no significant difference compared to wild type. These data corroborate that the reduction of free histidine in *cry-dash1*$_{mut}$ is due to the lack of CRY-DASH1.

Histidine is one of the proteinogenic amino acids. In plants, histidine was found to play an important role in growth and development.[39] In angiosperms and green algae, enzymes participating in the biosynthesis of histidine are localized in the chloroplast.[40] The histidine synthesis pathway starts with

Table 1 Chloroplast proteins downregulated in *cry-dash1*$_{mut}$ or only found in wild type SAG73.72.

Category		Name	NSAF	
			R 1	R 2
Glycolysis/ Gluconeogenesis	Cre02. g093450_4532	Fructose-1, 6-bisphosphate aldolase (FBA2)	0.6	o_wt
	Cre06. g262900_4532	Phosphofructokinase (PFK1)	0.6	o_wt
	Cre06. g278210_4532	Phosphoglucomutase 1 (PGM1)	0.5	0.7
	Cre10. g421700_4532	Glycerol-3-phosphate dehydrogenase/dihydroxyacetone-3-phosphate reductase (GPD4)	0.3	0.6
	Cre12. g485150_4532	Glyceraldehyde 3 phosphate dehydrogenase, chloroplastic (GAPC1)	0.6	o_wt
Dark fermentation	Cre01. g044800_4532	Pyruvate-formate lyase (PFL1)	0.6	0.7
	Cre09. g396650_4532	Phosphate acetyltransferase (PAT2)	0.1	0.4
	Cre12. g533550_4532	Pyruvate kinase 1 (PYK1)	0.3	0.6
Pentose phosphate pathway	Cre01. g032650_4532	Transaldolase (TAL1)	0.4	o_wt
	Cre12. g526800_4532	6-Phosphogluconate dehydrogenase, decarboxylating (GND1)	0.4	0.5
Acetate assimilation	Cre07. g353450_4532	Acetyl-CoA synthetase/ligase (ACS3)	0.2	0.7
Glyoxylate	Cre01. g042750_4532	Aconitate hydratase (ACH1)	0.7	0.5
	Cre03. g144807_4532	Malate synthase (MAS1)	0.4	0.5
Histidine biosynthesis	Cre09. g410650_4532	N-5-phosphoribosyl-ATP transferase (HIS1)	0.7	o_wt
	Cre11. g481500_4532	Imidazole glycerol phosphate synthase (HIS7)	0.4	0.7
Nitrate assimilation	Cre01. g007950_4532	Cytochrome P450, CYP55 superfamily, CYP55A family (CYP55B1)	0.6	0.2
	Cre13. g592200_4532	Glutamate synthase, NADH-dependent (GSN1)	o_wt	0.6
	Cre16. g655050_4532	NO-nitrate 1 (NON1)	o_wt	0.6
Ascorbate-gluthatione pathway	Cre02. g142200_4532	Glutathione S-transferase (GST5)	o_wt	0.6
	Cre06. g285150_4532	Ascorbate peroxidase-related (APX2)	o_wt	0.2
	Cre10. g456750_4532	Dehydroascorbate reductase (DAR1)	o_wt	o_wt
Starch metabolism	Cre07. g332300_4532	Alpha-glucan water dikinase 2 (GWD2)	0.7	0.4
	Cre17. g721500_4532	Granule-bound starch synthase IA (GBSS1A)	0.5	0.6
Aromatic amino acid biosynthesis	Cre13. g602350_4532	(1 of 1) K01609 – indole-3-glycerol phosphate synthase (trpC)*	0.6	0.3
	Cre14. g630859_4532	3-Hydroxyisobutyrate dehydrogenase (HID1)	o_wt	o_wt
	Cre17. g726750_4532	3-Deoxy-D-arabino-heptulosonate 7-phosphate synthetase (DHAPS1)	0.6	0.4
	Cre16. g694850_4532	N2-acetyl-L-ornithine:L-glutamate N-acetyltransferase (NAGS1)	0.7	0.5
PS related	Cre07. g328200_4532	PsbP-like protein of thylakoid lumen	0.7	0.3
	Cre10. g430150_4532	Low photosystem II accumulation 1 (LPA1)	0.5	o_wt
	Cre13. g564050_4532	(1 of 1) PTHR37764//PTHR37764:SF1 – family not named //MOG1/PSBP/ DUF1795-like Photosystem II reaction center psbP family protein*	0.7	o_wt

Table 1 (*continued*)

Category		Name	NSAF	
			R 1	R 2
Ribosomal proteins	Cre12.g512600_4532	Cytosolic 80S ribosomal protein L18 (RPL18)	0.7	0.6
	CreCp.g802300_4532	30S Ribosomal protein S18 (rps18)	0.7	0.7
	CreCp.g802303_4532	30S Ribosomal protein S9 (rps9)	0.7	0.6
Protein folding	Cre05.g241650_4532	(1 of 1) K01303 – Acylaminoacyl-peptidase [EC:3.4.19.1] (APEH)*	o_wt	o_wt
	Cre13.g577850_4532	Peptidyl-prolyl cis–trans isomerase, FKBP-type (FKB20)	0.6	0.7
Others	Cre01.g050150_4532	NADH:flavin oxidoreductase/NADH oxidase (NFO1)	0.5	o_wt
	Cre02.g097550_4532	(1 of 1) PTHR12532:SF0 – Transcriptional regulatory protein HAH1-related*	0.6	0.4
	Cre02.g143650_4532	Unknown protein	o_wt	o_wt
	Cre03.g197500_4532	Predicted protein (MOT6)	0.5	0.6
	Cre03.g203850_4532	ATP-sulfurylase (ATS1)	0.5	o_wt
	Cre06.g257000_4532	Sulfate binding protein, component of chloroplast transporter (SULP3)	0.6	0.7
	Cre06.g261750_4532	RuBisCO binding membrane protein 1 (RBMP1)	o_wt	0.6
	Cre06.g311850_4532	Halo-acid dehalogenase-like hydrolase	o_wt	o_wt
	Cre07.g327400_4532	NADH:ubiquinone oxidoreductase ND9 subunit (NUO9)	0.3	0.4
	Cre07.g335200_4532	Putative chloroplast TypA translation elongation GTPase (EFG12)	o_wt	0.6
	Cre08.g372000_4532	Chloroplast ATPase CF1 assembly factor (BAF3)	o_wt	o_wt
	Cre08.g380201_4532	Putative dehydroquinate dehydratase/shikimate:NADP oxidoreductase (SHKD1)	o_wt	0.6
	Cre10.g435300_4532	Aspartyl aminopeptidase-like protein (AAP1)	o_wt	0.5
	Cre11.g467767_4532	NADH:ubiquinone oxidoreductase 18 kDa subunit (NUO13)	0.6	0.6
	Cre12.g486100_4532	Active subunit of the chloroplast ClpP complex (CLPP5)	0.5	0.4
	Cre12.g519900_4532	(1 of 1) 6.3.2.13 – UDP-N-acetylmuramoyl-L-alanyl-D-glutamate-2,6-diaminopimelate ligase /UDP-N-acetylmuramyl-tripeptide synthetase*	0.3	0.4
	Cre12.g534250_4532	Unknown protein	0.6	0.5
	Cre12.g538700_4532	Conserved in the plant lineage and diatoms (CPLD62)	0.6	0.6
	Cre13.g569350_4532	NAD dependent epimerase/dehydratase	o_wt	o_wt
	Cre13.g603176_4532	(1 of 2) PTHR23023:SF4 – flavin-containing monooxygenase*	o_wt	o_wt
	Cre15.g801860_4532	(1 of 17) PF04755 – PAP fibrillin (PAP fibrillin)*	0.6	o_wt
	Cre16.g693500_4532	Hydroxyproline-rich flagellar associated protein 40 (FAP40)	o_wt	0.4
	Cre16.g694400_4532	Trigalactosyldiacylglycerol 2 (TGD2)	0.7	0.5
	Cre17.g698450_4532	(1 of 3) 3.5.4.9 – Methenyltetrahydrofolate cyclohydrolase*	0.6	o_wt
	Cre17.	Thioredoxin-like protein similar to Arabidopsis HCF164 (CCS5)	o_wt	0.4

(*continued on next page*)

Table 1 (*continued*)

Category	Name	NSAF	
		R 1	R 2
g702150_4532 Cre17. g739752_4532	Chloroplast-import FtsH-like ATPase (FTSHI1)	o_wt	0.7

Proteins inside the functional groups are sorted by their accession numbers according to Phytozome genome ID: 707 (*Chlamydomonas reinhardtii* CC-4532 v6.1). Gene symbols are put in parentheses; *, the auto defline is stated for proteins with no description; **NSAF**, normalized spectral abundance factor; **R1**, replicate 1; **R2**, replicate 2; **o_wt**, only found in wild type SAG73.72. CreCp numbers indicate genes that are encoded in the chloroplast, all others are encoded in the nucleus.

the amino acid precursor phosphoribosyl pyrophosphate (PRPP), which derives from the pentose phosphate pathway.[41] Therefore, the downregulation of the pentose phosphate pathway in *cry-dash1*$_{mut}$ may have a direct impact on the histidine biosynthesis pathway, resulting in a lower amount of histidine. It is important to note that histidine has been identified as a precursor in the biosynthesis of ovothiols. Ovothiols, which are 5(Nπ)-methylated thiohistidines, were recently discovered in marine diatoms and have been shown to exhibit potent antioxidant properties.[42] Consequently, the observed reduction in histidine levels in *cry-dash1*$_{mut}$ may increase the vulnerability to oxidative stress. One of the enzymes synthesizing ovothiols (UMM7) was recently found to be localized in the cilium in *C. reinhardtii*, indicating additional functions.[43] Moreover, histidine is an important amino acid in several photoreceptors of *C. reinhardtii* which belong to the His-kinase rhodopsins.[44] It remains open if these photoreceptors that can also have guanylate cyclase activity[45] are affected by CRY-DASH1.

CRY-DASH1 acts as a negative regulator of chlorophyll and carotenoid biosynthesis, of redox components and of some proteins of photosystem I and II

Several enzymes of chlorophyll biosynthesis are upregulated in *cry-dash1*$_{mut}$, resulting in a dark green phenotype of the mutant (Figure 2(A1) and (A2)). Intriguingly, cell growth is reduced in the mutant.[31] We found strong evidence that the reduction in growth is caused by shielding effects of the altered cell morphology of *cry-dash1*$_{mut}$ due to the excess of pigments and hyperstacking[31]. Thus, the light intensity in the middle of the culture is different in wild type and *cry-dash1*$_{mut}$. It is significantly reduced at day eight of the photoautotrophic growth in *cry-dash1*$_{mut}$ compared to wild type, even when the cell number of wild type is significantly higher compared to *cry-dash1*$_{mut}$ (Figure 2(A1)). Negative effects on the photosynthetic machinery by cell shading have been found before in microalgal cultures.[46]

The process of chlorophyll biosynthesis is complex and comprises around 30 structural genes and transcription factors.[47,48] The first precursor in chlorophyll biosynthesis pathway is 5-aminolevulinic acid. The initial steps of the pathway result in the formation of uroporphyrinogen III, which is the first cyclic tetrapyrrole (Figure 2(A2)). In one of the next steps, coproporphyrinogen III is converted to protoporphyrinogen IX, catalyzed by coproporphyrinogen III oxidase (CPX1), an enzyme that is upregulated in *cry-dash1*$_{mut}$ (Table 2, Figure 2 (A2)). The final chlorophyll branch starts with the insertion of a Mg^{2+} into protoporphyrin IX.[49] Two subunits of the Mg-chelatase (CHLH1 and CHLD1) that is catalyzing this step are upregulated. In case of the third subunit CHLI1, an increase in *cry-dash1*$_{mut}$ compared to wild type was only seen in one of the two replicates. As anti-CHLI1 antibodies are available, its regulation was verified by immunoblotting in three independent experiments. CHLI1 was confirmed to be upregulated in *cry-dash1*$_{mut}$ (Figure 2(B)). Moreover, we analyzed its amount in the complementing line 38, in which the level of CHLI shows no significant difference to wild type (Supplementary Figure 2). In barley, it was shown that the activity of the Mg-chelatase is induced by light *in vivo*.[50] Furthermore, in *A. thaliana,* light controls the redox state of CHLI in chloroplasts.[51] The last two steps of chlorophyll biosynthesis are catalyzed by POR1 and CHLG1 (Figure 2(A2), Table 2). Both enzymes are upregulated in *cry-dash1*$_{mut}$. POR1 is a key enzyme in the chlorophyll biosynthesis pathway that catalyzes the reduction of protochlorophyllide to chlorophyllide in a light-dependent manner.[52] In *C. reinhardtii*, the reduction of protochlorophyllide can also occur independently from light by the light-independent protochlorophyllide reductase, named chlL[47] that we did not identify among the changed proteins. CHLG1 is the final enzyme in the pathway for chlorophyll biosynthesis and is also upregulated in the mutant. Its role is to catalyze the process of esterification upon light exposure, which involves adding the hydrophobic phytol tail to the chlorophyllide.[53,54] The NADPH-dependent thioredoxin reductase (NTRC1), a regulator of Mg-protoporphyrin IX methyltransferase, is also upregulated in *cry-*

Table 2 Chloroplast proteins upregulated or only found in *cry-dash1*$_{mut}$ compared to wild type SAG73.72.

Category		Name	NSAF	
			R 1	R 2
Chlorophyll biosynthesis	Cre01.g015350_4532	Light-dependent protochlorophyllide reductase (POR1)	1.7	1.3
	Cre01.g054150_4532	NADPH-dependent thioredoxin reductase C, chloroplastic (NTRC1)	1.9	3.8
	Cre02.g085450_4532	Coproporphyrinogen III oxidase (CPX1)	2.1	1.7
	Cre05.g242000_4532	Magnesium chelatase subunit D, chloroplast precursor (CHLD1)	3.7	2.3
	Cre06.g294750_4532	Chlorophyll synthetase (CHLG1)	o_mut	o_mut
	Cre07.g325500_4532	Magnesium chelatase subunit H (CHLH1)	2.4	1.7
Redox	Cre11.g476750_4532	Ferredoxin-NADP reductase, chloroplast (FNR1)	1.3	1.4
	Cre12.g496700_4532	Thioredoxin-like protein	o_mut	o_mut
	Cre12.g513750_4532	Glutaredoxin, CPYC type (GRX1)	2.3	o_mut
	Cre12.g553700_4532	Protein disulfide oxidoreductase (PDO2)	1.6	1.7
PS related	Cre06.g273700_4532	Photosystem II stability/assembly factor (HCF136)	2.1	1.5
	Cre07.g330250_4532	Photosystem I reaction center subunit H (PSAH1)	1.4	1.5
	Cre09.g411200_4532	PSII assembly protein (PSB33)	2.7	1.4
	Cre12.g560950_4532	Photosystem I reaction center subunit V (PSAG1)	1.8	1.8
Carotenoids biosynthesis	Cre12.g484200_4532	Geranylgeranyl pyrophosphate synthase, putative chloroplast precursor (GGPS1)	o_mut	2.3
	Cre12.g503550_4532	2-C-methyl-D-erythritol 2, 4-cyclodiphosphate synthase (MEC1)	o_mut	o_mut
	Cre12.g509650_4532	Phytoene desaturase (PDS1)	2.5	2.8
Photoprotection	Cre03.g146167_4532	Homolog of hypersensitive to high light 1 (HHL1)	1.9	1.6
	Cre09.g393173_4532	Early light-induced LHC-like protein (ELIP8)	2.4	2.6
Acyl-lipid metabolism	Cre03.g189300_4532	Plastid lipid associated protein 10 (PALP10)	1.6	2.6
	Cre13.g577100_4532	Acyl-carrier protein 2 (ACP2)	1.8	1.6
	Cre13.g590500_4532	Omega-6-fatty acid desaturase, chloroplast isoform (FAD6)	1.5	o_mut
	Cre14.g618050_4532	Plastid lipid associated protein 3 (PLAP3)	1.9	o_mut
Amino acid and polyamine metabolism	Cre01.g015000_4532	N-acetyl-l-glutamate kinase (NAGK1)	1.7	1.8
	Cre02.g107300_4532	Dihydrodipicolinate synthase (DPS1)	o_mut	o_mut
	Cre10.g436350_4532	Shikimate kinase (SHKF1)	o_mut	3.3
	Cre12.g501050_4532	Aldehyde dehydrogenase	o_mut	o_mut
	Cre12.g507558_4532	(1 of 1) 3.5.1.3 – Omega-amidase*	o_mut	2
	Cre12.g558450_4532	Spermidine synthase (SPD1)	o_mut	o_mut

(*continued on next page*)

Table 2 (*continued*)

Category		Name	NSAF	
			R 1	R 2
Transcription	Cre06.g274650_4532	Complex I intermediate-associated CIA30 protein, mitochondrial (NUOAF4)	1.6	1.3
	Cre14.g610501_4532	Short-chain dehydrogenase/reductase found in psaA trans-splicing complex (RAA14)	1.5	2.2
Translation	Cre06.g278086_4532	(1 of 1) PTHR11803//PTHR11803:SF17 – Translation initiation inhibitor //subfamily not named*	o_mut	o_mut
	Cre07.g341850_4532	Chloroplast translation initiation factor 2 (CIF2)	2.4	o_mut
	Cre16.g654500_4532	Eukaryotic translation initiation factor 3, subunit F (EIF3F)	1.5	o_mut
Conserved in plant lineage	Cre02.g141100_4532	Conserved in the plant lineage (CPL23)	1.9	2.2
	Cre08.g379200_4532	Conserved in the plant lineage and diatoms (CPLD18)	1.5	1.6
Ribosomal proteins	CreCp.g802277_4532	50S ribosomal protein L14 (rpl14)	1.5	2.5
	CreCp.g802283_4532	30S ribosomal protein S4 (rps4)	1.3	1.7
Protein folding	Cre07.g315700_4532	Peptidyl-prolyl cis–trans isomerase, FKBP-type (FKB16A)	o_mut	o_mut
	Cre12.g561000_4532	Cyclophilin 28 (CYN28)	1.4	1.4
	Cre16.g675550_4532	Peptidyl-prolyl cis–trans isomerase, FKBP-type (FKB16B)	1.7	1.7
Others	Cre01.g016300_4532	Calmodulin-like protein	2.9	2
	Cre02.g142351_4532	(1 of 2) K15631-Molybdenum cofactor sulfurtransferase (ABA3)*	1.9	1.4
	Cre03.g145247_4532	S-isoprenylcysteine O-methyltransferase (TEF11)	1.6	o_mut
	Cre03.g177500_4532	(1 of 2) K17279 – Receptor expression-enhancing protein 5/6 (REEP5_6)*	o_mut	2.6
	Cre04.g226850_4532	Pepsin-type aspartyl protease (ASP1)	1.9	2.8
	Cre05.g240800_4532	NADH:ubiquinone oxidoreductase 17 kDa subunit (NUO17)	1.5	1.5
	Cre06.g270100_4532	Starch branching enzyme 2 (SBE2)	1.5	o_mut
	Cre06.g800656_4532	(1 of 4) PTHR16222//PTHR16222:SF17 – ADP-ribosylglycohydrolase //subfamily not named*	1.4	2.2
	Cre07.g323600_4532	(1 of 1) PF11317 – Protein of unknown function (DUF3119)*	1.6	o_mut
	Cre08.g370650_4532	6-Phosphogluconolactonase (PGL2)	1.4	1.7
	Cre09.g394850_4532	LrgB-like protein (TEF24)	o_mut	o_mut
	Cre09.g410250_4532	Unknown protein	1.6	1.4
	Cre10.g452350_4532	Unknown protein	1.9	o_mut
	Cre10.g458550_4532	Chloroplast protein biogenesis factor (STIC2)	o_mut	o_mut
	Cre11.g467535_4532	Mitochondrial substrate carrier protein	o_mut	1.5
	Cre11.g467778_4532	(1 of 1) K00761 – uracil phosphoribosyltransferase (upp, UPRT)*	1.8	1.6
	Cre12.g516450_4532	Gamma carbonic anhydrase 1 (CAG1)	o_mut	o_mut

Table 2 (*continued*)

Category		Name	NSAF	
			R 1	R 2
	Cre12.g556250_4532	Septin-like protein	o_mut	o_mut
	Cre13.g586050_4532	(1 of 1) PTHR13833:SF49 – NHL repeat-containing protein 2*	o_mut	2.1

Proteins inside the functional groups are sorted by their accession numbers according to Phytozome genome ID: 707 (*Chlamydomonas reinhardtii* CC-4532 v6.1). Gene symbols are put in parentheses; *, the auto defline is stated for proteins with no description; **NSAF**, normalized spectral abundance factor; **R1**, replicate 1; **R2**, replicate 2; **o_mut**, only found in *cry-dash1*$_{mut}$. CreCp numbers indicate genes that are encoded in the chloroplast, all others are encoded in the nucleus.

dash1$_{mut}$. It was shown that NTRC1 plays a crucial role in the redox modulation under low light conditions, as well as in protecting plants from photooxidative damage.[55,56] In this context it is also noteworthy to mention that four components of redox regulation each belonging to a different group of redox proteins (thioredoxins, glutaredoxins, protein disulfide isomerases and ferredoxins[57] are upregulated in *cry-dash1*$_{mut}$ (Table 2). Taken together, light and redox regulation are closely linked with chlorophyll biosynthesis. CRY-DASH1 obviously plays an important role as negative regulator in these processes. Also in carotenoid biosynthesis, three key enzymes of the pathway are upregulated, being geranylgeranyl pyrophosphate synthase (GGPS1), 2-C-methyl-D-erythritol 2,4-cyclodiphosphate synthase (MEC1) and phytoene desaturase (PDS1).[58]

Beside the above-mentioned pathways, certain proteins of PSII and PSI are also upregulated in the mutant (Figure 2(A3), Table 2).[31] Thus, PSAH1 and PSAG1 of PSI are increased in the mutant. They are connected to supercomplex formation, are known to be parts of the light harvesting chlorophyll *a/b* complex I and can be involved in state transitions.[59–61]

In case of PSII, the PSII assembly protein PSB33 that is known to be part of a UV-A-light-triggered mechanism to sustain a functional PSII in plant chloroplasts[62] is increased in the mutant. This is of interest as CRY-DASH1 has its absorption peak in the UV-A range. Moreover, the PSII stability/assembly factor HCF136 (High Chlorophyll Fluorescence136) was found to be increased. The luminal protein is necessary for inserting the nascent central D1 protein into the reaction center.[63–65] Studies about the presence of this factor in chloroplast membranes resulted in the hypothesis that chloroplasts may have diverse biogenic membranes.[66] Two other PSII proteins, D1 and its antenna protein CP43 were only found clearly upregulated in one replicate in this study. However, they have been verified before by immunoblots in three independent experiments and were found to be upregulated in the mutant[31] (Figure 2(A3)). In contrast, the two other central proteins of PSII, D2 (Supplementary Figure 3) and CP47[31] are not differentially expressed in wild type and *cry-dash1*$_{mut}$ as verified by immunoblots. We also analyzed the PSI/PSII ratio and found that there is no significant difference between wild type and *cry-dash1*$_{mut}$ (Figure 2(A4) and Supplementary Figure 4).

It is unexpected that only D1 and its antenna protein CP43 are upregulated, but not D2 and CP47. As there are two CRY-DASH proteins encoded in *C. reinhardtii*, one hypothesis is that both CRY-DASH proteins may have partially overlapping functions and CRY-DASH2 may control further proteins of PSII. Such a postulation must be carefully analyzed in the future. Altogether our data indicate that only some proteins of the photosynthetic machinery are upregulated in *cry-dash1*$_{mut}$; some proteins of PSII are even downregulated (Supplementary Table 5). Among the upregulated proteins, CP43 as well as an early light inducible LHC (ELIP8) have the capacity to integrate chlorophyll molecules. ELIPs are located in the thylakoid membrane and protect the photosynthetic machinery from stresses such as cold induced photooxidative stress.[67] The increase in an ELIP may thus be related to stress effects realized by the changes of the photosynthetic machinery in *cry-dash1*$_{mut}$.

PSII biogenesis of D1 is regulated by light in *A. thaliana*, involving the cryptochrome and phytochrome photoreceptors.[68] In this process, HCF173, which initiates D1 translation, is involved as well as the luminal HCF136, as modelled recently.[68–70] HCF173 of *C. reinhardtii* is not included in Tables 1 and 2, as it was found in one replicate with two peptides but in the other one with only one peptide. However, we would like to mention that these peptides were only found in the mutant in both replicates (see Supplementary Tables 1–4(A)); thus, HCF173 that is relevant for D1 translation seems upregulated in the mutant. We were interested to find out whether there may be some coregulation of D1 and the CRY-DASH1 photoreceptor in *C. reinhardtii*. It is known that translation of chloroplast encoded D1 by *psbA* mRNA is modulated in the light.[71] Also, it has become evident that the synthesis of D1 is highly complex involving co-translational chlorophyll association to nascent D1.[70] To study a potential interplay between D1 and CRY-DASH1, we used a D1

deletion mutant that was grown mixotrophically in TAP medium (see Methods) as done before.[70] We compared the protein expression level of CRY-DASH1 in the D1 mutant cells and the corresponding wild type 137c during daytime (LD6; 6 hours after light has been switched on in a 12:12 h light–dark cycle) and nighttime (LD18; 6 hours after light has been switched off in a 12:12 h light–dark cycle). The protein amount of CRY-DASH1 was significantly increased in the D1 deletion mutant at both time points (Figure 2(C)), suggesting that D1 and CRY-DASH1 are regulating each other through a feedback loop. It remains open whether coupling of *psbA* translation to light-induced D1 damage[69] may be connected to this regulation in the green alga *C. reinhardtii*. But the intriguing finding that CRY-DASH1 uses light not only as a source of information but connects this information with energy metabolism, may open new routes in the future for biotechnological approaches.

CRY-DASH1 seems to act at the posttranscriptional/translational level

It was shown before that the blue light receptor phototropin acts in a positive way on chlorophyll biosynthesis in *C. reinhardtii*.[72] This occurs at the transcript level. To find out whether CRY-DASH1 may also act at the transcriptional level in chlorophyll biosynthesis, we analyzed mRNA levels of several genes that encode enzymes upregulated

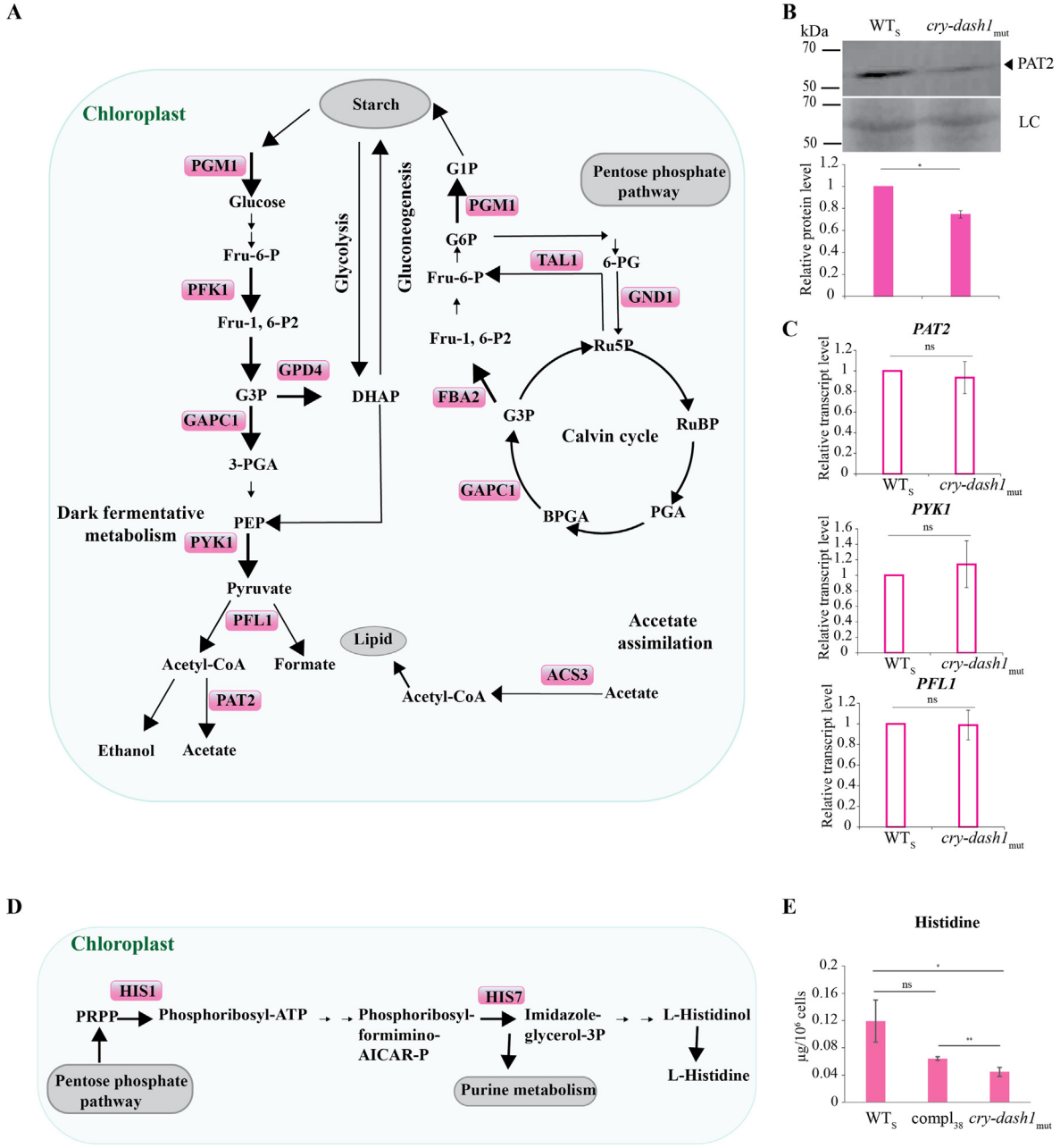

in the mutant, including *CHLI1*, *CHLH1*, *CHLD1* and *CHLG1*. In none of these cases, the amount of mRNA was increased in *cry-dash1*$_{mut}$ compared to wild type. Either it was similar or even slightly downregulated in the mutant (Figure 2(D) and Supplementary Figure 5). This data clearly suggests that CRY-DASH1 acts at the posttranscriptional/translational level as also found for the selected downregulated proteins PAT2, PYK1 and PFL1 as well as for upregulated D1 and CP43. Their RNAs are similar in wild type and mutant (31, Figure 1 (C), Figure 2(E)). As mentioned before, *psbA* mRNA encoding D1 is under translational control and its translation is modulated by light.[71] CRY-DASH1, which is encoded in the nucleus and has a chloroplast target sequence, is found in the chloroplast fraction by immunoblots (Supplementary Figure 1(A)).[31] It may directly act on the plastidial *psbA* mRNA. Currently, we do not know whether CRY-DASH1 is also present in the cytoplasm. Thus, we assume that CRY-DASH1 could act via retrograde signaling to control posttranscriptional/translational regulation in the cytoplasm of nuclear encoded genes such as *CHL*s, *PAT2* etc. in a positive or negative manner. Plastidial signaling components or metabolites such as Mg protoporphyrin-IX could hereby serve as signals.[73]

As CRY-DASH1 bears four "RGG" RNA-binding motifs at its C-terminus, it seems likely that CRY-DASH1 may indeed directly interact with RNA. RGG motifs can be involved, for example, in mRNA translational repression.[74,75] Light has been formerly proposed to stimulate the translation of *psbA* mRNA also in *C. reinhardtii* by activating a protein complex associated with the 5'-UTR of this mRNA.[76,77] We thus took *psbA* RNA and checked whether CRY-DASH1 can bind to it. For this purpose, we used an *in vitro* RNA-binding assay (modified from 78 along with a CTP-biotinylated transcript including the 5'-UTR and 191 bp of the open reading frame of *psbA* RNA (Supplementary Figure 6),[76] that was bound to paramagnetic streptavidin beads. As a control, we used the 3'-UTR of *glutamine synthetase2* mRNA (*GS2*) that is recognized by the heteromeric RNA binding protein CHLAMY1.[78] Yeast RNA was added as non-specific competitor RNA in the first five washing steps (see Methods; Figure 2 (F)). Heterologously expressed CRY-DASH1[31] was used for the assay; it had been purified by Ni- and heparin-affinity chromatography followed by a centrifugal filter step with a size exclusion of 50 kDa (see Methods). Thus, removal of potentially co-isolated Hfq from *E. coli*, which was reported to have RNA binding properties,[79] was ensured via the size exclusion step.

We found that CRY-DASH1 binds efficiently to *psbA* RNA *in vitro* (Figure 2(G)). There was no unbound CRY-DASH1 left in the supernatant and in the eluate a strong CRY-DASH1 signal was observed in immunoblots using anti-CRY-DASH1 antibodies. In contrast, CRY-DASH1 was still present unbound in the supernatant with the control *GS2* transcript, and it was not visible in the control *GS2* transcript after the washing steps with non-specific yeast RNA (Figure 2(G)). These results suggest that CRY-DASH1 binds selectively to the 5'-end of the *psbA* RNA and corroborate that CRY-DASH1 acts at the posttranscriptional level, possibly by controlling translation through its direct binding to involved RNAs. In this case, CRY-DASH1 seems to exert a repressor function as its absence results in a higher amount of the encoded D1 protein. One possibility is that CRY-DASH1 might act as a competitor of HCF173 that promotes translation of *psbA* RNA in the chloroplast[68] as outlined in the graphical abstract. Here, yet unknown additional factor(s) could also play a role.

A dual role of photoreceptors as activators or repressors in individual processes is also known

Figure 1. Several enzymes of central carbon and histidine metabolism are downregulated in *cry-dash1*$_{mut}$. (A) The main enzymes which are downregulated are shown with magenta boxes as well as relevant metabolites. (PGM1, Phosphoglucomutase 1; PFK1, Phosphofructokinase; GPD4, Glycerol-3-phosphate dehydrogenase; GAPC1, Glyceraldehyde 3-phosphate dehydrogenase; TAL1, Transaldolase; GND1, 6-phosphogluconate dehydrogenase; FBA2, Fructose-1,6-bisphosphate aldolase; PYK1, Pyruvate kinase 1; PFL1, Pyruvate-formate lyase; PAT2, Phosphate acetyltransferase; ACS3, Acetyl-CoA synthetase/ligase); Fru-P, Fructose-phosphate; GP, Glyceraldehyde-phosphate; PGA, Phosphoglycerate; PEP, Phosphoenolpyruvate; Ru5P, Ribulose-5-phosphate; RuBP, Ribulose-1,5-bisphosphate; BPGA, Bisphosphoglycerate.[36] (B) Cultures were harvested at LD8 (8 h after the light has been switched on). 100 μg of total protein were separated by 10% SDS PAGE and immunoblotted with anti-PAT2 antibodies. Selected bands from a nitrocellulose membrane stained with Ponceau S were used as loading control (LC). (C) Relative transcript levels of *PAT2*, *PYK1* and *PFL1* in wild type (WT) and *cry-dash1*$_{mut}$ (Mut) analysed by quantitative RT-PCR using *RACK1* as internal reference gene. (D) Simplified histidine pathway where the downregulated enzymes are shown with magenta boxes. (HIS1, N-5-phosphoribosyl-ATP transferase; HIS7, Imidazole glycerol phosphate synthase; PRPP, phosphoribosyl pyrophosphate; AICAR-P, aminoimidazole carboxamide ribonucleotide monophosphate). (E) The amount of free histidine measured by HPLC in WT, *cry-dash1*$_{mut}$ and the complementing line compl$_{38}$ that expresses CRY-DASH1 up to 53% are shown. For quantification, the protein levels in wild type were normalized to 1 and compared with the levels in the mutant. $n = 3$ biological replicates; error bars represent SD; asterisks indicate significant differences as estimated by the Student's *t*-test (*, $P < 0.05$; **, $P < 0.01$; ns, not significant).

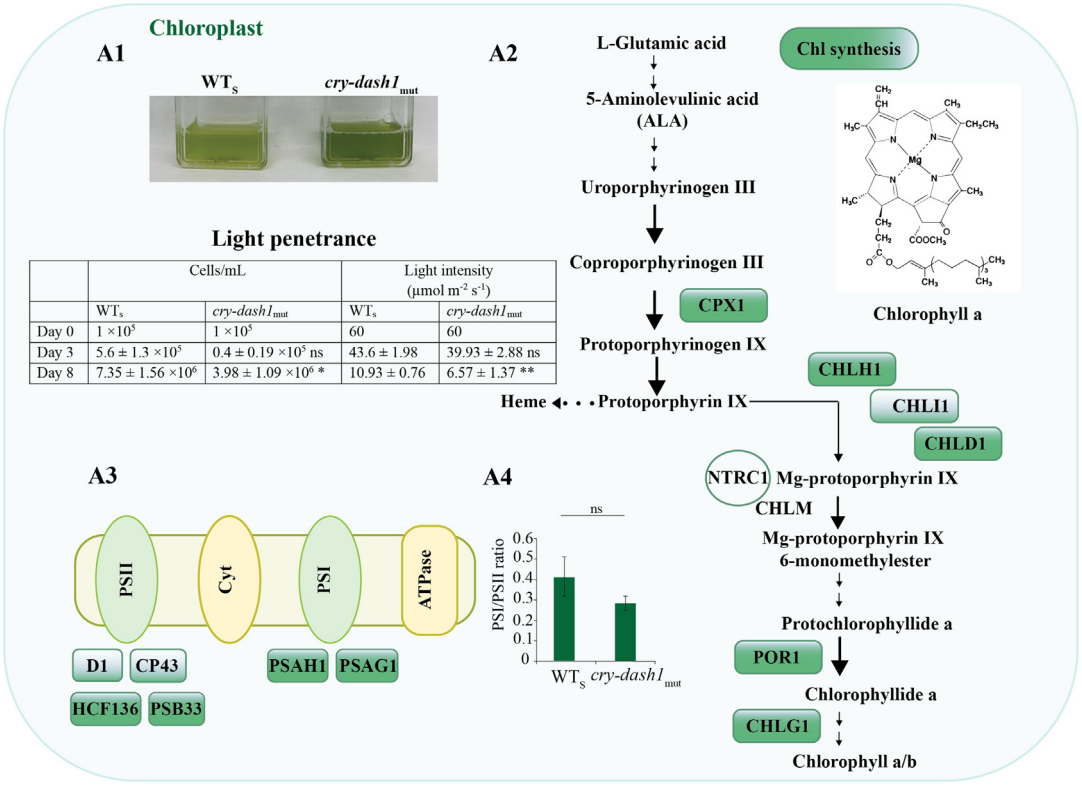

	Cells/mL		Light intensity (µmol m^{-2} s^{-1})	
	WTs	*cry-dash1*mut	WTs	*cry-dash1*mut
Day 0	1 ×10^5	1 ×10^5	60	60
Day 3	5.6 ± 1.3 ×10^5	0.4 ± 0.19 ×10^5 ns	43.6 ± 1.98	39.93 ± 2.88 ns
Day 8	7.35 ± 1.56 ×10^6	3.98 ± 1.09 ×10^6 *	10.93 ± 0.76	6.57 ± 1.37 **

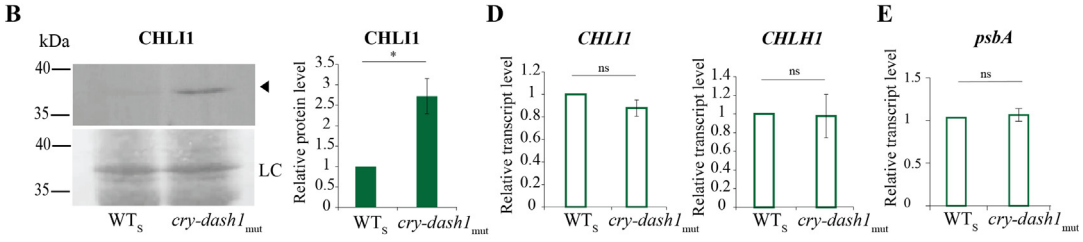

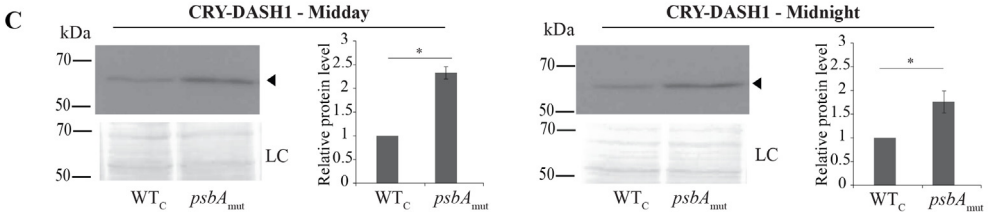

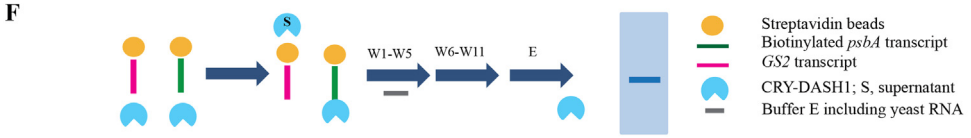

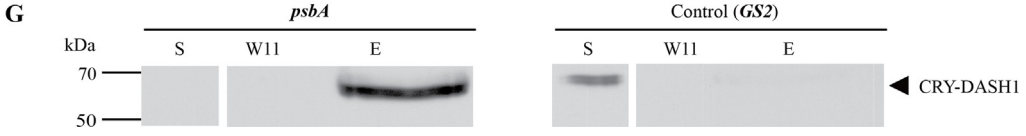

from other cryptochromes. Thus, pCRY and aCRY act as negative elements in the gametogenesis process of *C. reinhardtii*, while both are positive regulators for its germination.[21,22] The blue light photoreceptor phototropin of *C. reinhardtii* is even multifunctional. It promotes different steps in the sexual life cycle,[80] it is involved in eyespot development and in phototactic behavior,[81] mediates feedback regulation of photosynthesis[82] and also influences photoprotection and the CO_2 concentrating mechanism.[83] It will be intriguing to find out in the future whether these photoreceptors might be part of a functional network.

Materials and Methods

Strains and culture conditions

C. reinhardtii strain SAG73.72 (mt^+) obtained from the 'Sammlung von Algenkulturen in Göttingen' was used as wild type. A transgenic *C. reinhardtii* line lacking the CRY-DASH1 protein, named *cry-dash1*$_{mut}$ (LMJ.RY0402.181834, mt^-) that was backcrossed three times into SAG73.72 was used for functional comparisons.[31] Main algal cultures were grown photoautotrophically in minimal medium prepared basically according to Levine and Ebersold.[84] Briefly, 899 mL H_2O were mixed with 50 mL Beijerinck's solution (13 g/L NH_4Cl, 1 g/L $CaCl_2 \times 2\ H_2O$, 2 g/L $MgSO_4 \times 7\ H_2O$) and 1 mL Hutner's trace elements[85] and then 50 mL phosphate buffer (14.34 g K_2HPO_4, 7.26 g KH_2PO_4) were added. Cells were grown under a 12 h: 12 h, light–dark (LD) cycle with a light intensity of 60 μmol m^{-2} s^{-1} (Osram L36W/840, lumilux, cool white) at 23 °C and harvested at LD4 unless otherwise indicated. LD0 defines the start of the light regime and LD12 the start of the dark regime. LD4 means that the light has been switched on for 4 h. In the case of the *psbA* deletion mutant *FuD7* (CC4147, mt^+) that was obtained from the *Chlamydomonas* resource center and its corresponding wild-type strain 137c (mt^+), cultures were grown in Tris-Acetate-Phosphate (TAP) medium.[85] The *FuD7* mutant and its wild type were harvested at midday (LD6) and midnight (LD18), respectively. Light measurements were carried out using a LI-189 quantum radiometer photometer (LI-COR).

Light measurements within the algal cell culture

Cultures were adjusted to a cell number of 1×10^5 cells/mL and grown photoautotrophically

Figure 2. Several enzymes of chlorophyll biosynthesis are upregulated in *cry-dash1*$_{mut}$. (A1) On the top left an exemplary culture of the wild type SAG73.72 (WT_S) and the mutant (*cry-dash1*$_{mut}$) are shown; the cell number was adjusted to 5×10^6 cells/mL. Below, photoautotrophic cell growth of WT_S and *cry-dash1*$_{mut}$ from day 0, day 3 and day 8 is indicated as cells/mL and the light intensity in the culture (see Methods) in shown. (A2, 3) Enzymes which are upregulated in *cry-dash1*$_{mut}$ are shown with green boxes. Enzymes that are upregulated in only one replicate (31, Figure 2(B)) and verified by immunoblots are shown in light green boxes. The enzyme regulator NTRC1 is shown with a circle. (CPX1, Coproporphyrinogen III oxidase; CHLD1, CHLI1, CHLH1, Mg-chelatase; POR1, Light-dependent protochlorophyllide reductase; CHLM, Mg-protoporphyrin IX methyltransferase; CHLG1, Chlorophyll synthetase; NTRC1 regulator, NADPH-dependent thioredoxin reductase C. The chlorophyll pathway and the formula were adapted from 46; 91. (A3) Up-regulated components of the photosystems: D1 of PSII and its antenna protein CP43; both are encoded in the chloroplast in contrast to all other candidates of (A2) and (A3) that are encoded in the nucleus. PSB33, PSII assembly protein; HCF136, Photosystem II stability/assembly factor; PSAH1; Photosystem I reaction center subunit H; PSAG1, Photosystem I reaction center subunit V) (A4) PSI to PSII ratio from WT and *cry-dash1*$_{mut}$. The corresponding immunoblots are shown in Supplementary Figure 4. (B) 100 μg of total protein were separated by 10% SDS-PAGE and immunoblotted with anti-CHLI antibodies. Selected bands from a nitrocellulose membrane stained with Ponceau S are used as a loading control (LC). (C) CRY-DASH1 level in WT_C (137C, mt^+) and a *psbA* deletion mutant (CC4147, mt^+). 50 μg of total protein were separated using a 10% SDS gel and immunoblotted with anti-CRY-DASH1 antibodies. Selected bands from a PVDF membrane stained with Coomassie Brilliant Blue R250 are used as a loading control (LC). (D, E) Relative transcript levels of *CHLI1* and *CHLH1* (D) and *psbA* (E), respectively, in WT_S and *cry-dash1*$_{mut}$ analyzed by quantitative RT-PCR using *RACK1* as internal reference gene.[31] (F) Schematic view of the *in vitro* RNA binding assay with purified RNA-binding proteins. Biotinylated transcripts were bound to the magnetic beads coated with streptavidin. Target proteins were bound to the RNA, washed in the presence of competitor RNA and eluted from the beads (see Methods). Elution was checked by immunoblot with the antibodies against the target proteins. (G) *In vitro* RNA binding assay using biotinylated *psbA* 5'-end (*psbA*) or *glutamine synthetase2* 3'-end containing seven UG repeat (*GS2*) indicates that CRY-DASH1 binds selectively to *psbA* 5'-end. Biotin-14-CTP labelled *psbA* or *GS2* transcripts were bound to the streptavidin beads and incubated with purified His-tagged CRY-DASH1 protein (1 μg). 80 μL of the supernatant (S) representing unbound CRY-DASH1, last washing steps (W11), and elution (E) were separated by 10% SDS-PAGE and immunoblotted with anti-CRY-DASH1 antibody. For quantification, the protein levels in wild type were normalized to 1 and compared with the levels in the mutant. $n = 3$ biological replicates; error bars represent SD; asterisks indicate significant differences as estimated by the Student's *t*-test (*, $P < 0.05$; **, $P < 0.01$; ns, not significant).

as described above. Measurement of the light intensity in μmol m^{-2} s^{-1} inside the cultures was performed by using the US-SQS spherical quantum sensor (Walz GmbH, Effeltrich, Germany), which was placed in the middle of each tube.

Chloroplast isolation and protein extraction

Chloroplast fractions of strains, SAG73.72 and *cry-dash1*$_{mut}$ were isolated as described.[31,32] Briefly, 1 L of SAG73.72 and *cry-dash1*$_{mut}$ cultures were precultured in TAP with a cell concentration of 1 × 10^5 cells/mL and were grown until they reached the cell concentration of 5 × 10^6 cells/mL and harvested at LD4. Cells were then transferred to minimal medium[84] and exposed to high light (ca. 150 μmol m^{-2} s^{-1}) as described to ensure synchrony of cells.[32] They were grown until they reached a density of 8 × 10^6 cells/mL. As SAG73.72 and *cry-dash1*$_{mut}$ strains have a cell wall, cells were treated with 50 mL autolysin (prepared according to 85) for up to two hours prior to chloroplast extraction. The autolysin treated cells were centrifuged at 3,000*g* for 5 min at 4 °C and resuspended in 2 mL of 50 mM HEPES-KOH (pH 7.5) by gentle pipetting. All the following steps were carried out at 4 °C. The suspension was diluted with 8 mL isolation buffer (300 mM sorbitol, 50 mM HEPES–KOH (pH 7.5), 2 mM Na-EDTA (pH 8.0), 1 mM $MgCl_2$ × $6H_2O$, 1% BSA). Cells were rapidly squeezed into a syringe with a 27-gauge needle at a flow rate of 0.1 mL s^{-1} and crude chloroplasts were collected by centrifugation at 750*g* for 2 min at 4 °C. Pellets were resuspended in 2 mL of isolation buffer using a fine paintbrush to avoid disrupting the chloroplasts. The suspension was overlaid at the top of the Percoll gradient and was centrifuged for 20 min at 4,000*g* without braking. The chloroplast fraction was taken at the interface between 45% and 65% Percoll and diluted with 10 mL isolation buffer. The suspension was centrifuged (680*g* for 1 min at 4 °C) and the supernatant was removed. The pellet was resuspended in isolation buffer to a final volume of 3 mL and used for a second Percoll gradient. The final obtained fractions were rinsed once with isolation buffer and twice with 250 μL of 50 mM HEPES-KOH pH 8.0 + 0.3 M sorbitol. The proteins were extracted by adding 200 μL of 2 × SDS sample buffer (100 mM Tris-Cl, pH 7.5, 200 mM DTT, 4% (w/v) SDS, 0.2% (w/v) Bromophenol Blue, 20% (w/v) glycerol) and incubating for 5 min at 80 °C.

Mass spectrometry sample preparation

For MS analysis, proteins were separated in a 10% AA-PDA (acrylamide-piperazine diacrylamide) gel, prepared with MS-Grade solutions. The gel was stained for a maximum of 12 h with Novex Colloidal Blue Staining Kit (Thermo Fisher Scientific) following the protocol of the supplier. The gel was destained overnight with ddH_2O and 12 gel bands from each lane were excised and washed with wash solution A (10 mM ammonium hydrogen carbonate) and subsequently with wash solution B (5 mM ammonium hydrogen carbonate in 50% acetonitrile) until the gel pieces were completely destained. Proteins from each gel piece were digested with sequencing-grade modified trypsin (Promega) at 37 °C overnight and the resulting peptides were desalted with ZipTip-columns (Merck Millipore) supplemented with additional Poros R2 10 μm (Applied Biosystems) as described before.[86]

Liquid chromatography electrospray ionization tandem mass spectrometry (LC-ESI-MS/MS)

Dried peptides were resuspended in a solution containing 5% (v/v) DMSO and 5% (v/v) formic acid and subjected to nano-LC-ESI-MS/MS using an UltiMate 3000 nano UHPLC (Thermo Fisher Scientific) with a flow rate of 300 nL min^{-1} coupled online with a Thermo Fisher Scientific Q Exactive Plus mass spectrometer. Peptides were separated on a Acclaim PepMap 100 C18 column (75 μm inner diameter × 15 cm, 2 μm particle size; Thermo Fisher Scientific) using a 1 hour gradient with the following specifications: 5 min 96% A/4% B (v/v); within 1 min gradually to 10% B (v/v); within 34 min gradually to 55% A/45% B (v/v); within 2 min gradually to 95% B (v/v); 6 min 95% B (v/v); within 1 min gradually to 96% A/4% B (v/v); 11 min 96% A/4% B (v/v) whereby A consists of 0.1% (v/v) formic acid in water and B consists of 0.1% (v/v) formic acid in 80% acetonitrile. Ions were introduced by positive electrospray ionization and mass spectra were acquired over *m*/*z* 300–1,750 at 70,000 resolution (*m*/*z* 200) using an automatic gain control (AGC) target of $1e^6$. The top 10 most abundant precursor ions with positive charge states of 2–7 were selected for tandem MS by higher-energy collisional dissociation (HCD) fragmentation. For HCD, an isolation width of 1.6 *m*/*z*, a maximum fill time of 110 ms, and an AGC target of $1e^5$ was used. These selected precursor masses were excluded from the analysis for 20 s after each cycle. Peptides were fragmented by a normalized collisional energy of 30, and fragment spectra acquired at a resolution of 17,500 (*m*/*z* 200).

Data analysis

Raw data files were processed with the Proteome Discoverer software (version 2.4; Thermo Fisher Scientific) using the SEQUEST algorithm.[87] Data were searched against the *C. reinhardtii* database v6.1 hosted by Phytozome (Vs13) (https://phytozome-next.jgi.doe.gov/). Searches were done for tryptic peptides, allowing two missed cleavages.

Search parameters included oxidized methionine as a variable modification. Assignments were made using a 10 ppm mass tolerance for the precursor and 0.02 Da mass tolerance for the fragments. The search parameters were set to achieve a false discovery rate (FDR) of 1%.

Mass spectrometry-based relative quantification

For the mass spectrometry-based relative quantification of proteins we used the normalized spectral abundance factor (NSAF)[34,35] for comparing the protein abundance between *cry-dash1*$_{mut}$ and wild type. Briefly, the total number of identified peptides per protein represented as spectral counts (SpC) was divided by its number of amino acids (L). To determine the relative abundance, the ratio SpC/L was divided by the sum of SpC/L for all identified proteins for the *cry-dash1*$_{mut}$ sample and for the corresponding wild-type sample, respectively. Thereafter, the NSAF of each individual protein of the *cry-dash1*$_{mut}$ sample was divided by the corresponding NSAF of the wild-type sample to determine if the abundance of proteins is increased or decreased. Proteins were classified as upregulated in *cry-dash1*$_{mut}$ if the ratio of the NSAF of each individual protein of *cry-dash1*$_{mut}$ sample to the NSAF of the wild-type sample was equal or above to 1.33 and classified as downregulated in *cry-dash1*$_{mut}$ if the ratio was equal or below to 0.75.

Extraction of free amino acids from C. reinhardtii

The experiments were performed according to 88 with some modifications. 5 mL of algal cultures were grown photoautotrophically as described above and collected in exponential phase at LD4, centrifuged (5 min, 5,000*g*) and washed twice with HPLC grade water (Roth). Free amino acids from the algae were extracted in 200 μL of hot (80 °C) HPLC grade water, incubated at 80 °C for 30 min and centrifuged. The supernatant was collected in a new tube and the pellet was re-extracted with 200 μL of HPLC grade water. The supernatant was then collected and used for pre-column derivatization.

HPLC analysis of free amino acids from C. reinhardtii

The analyzation of free amino acids was done as described[88] with the following specifications. A O-Phthaldialdehyde (OPA) pre-column (Sigma–Aldrich) derivatizing agent was prepared by dissolving 0.135 g in 5 mL methanol (HPLC grade) and made up to 25 mL with borate buffer (0.1 M). On the day of use, 10 μL of 2-mercaptoethanol was added to 1.5 mL OPA stock solution. The reaction was started by the addition of 10 μL derivatization reagent to 40 μL of sample and the mixture was shaken. After 1 min the reaction was halted by the addition of 25 μL of boric acid (0.4 M) and shaken. 20 μL of sample were injected onto the HPLC (HPLC Agilent 1220 Infinity, Agilent Technologies) exactly 2 min after the start of the derivatization. For amino acid detection, two mobile phases were used: (A) 0.05 M sodium acetate (pH 6.8): methanol (9:1 v/v) plus 2% tetrahydrofuran (THF); (B) methanol plus 0.5% THF. The flow rate was 1.2 mL min^{-1}. The gradient was 0% B at 0 min, 52% B at 14 min, 80% B at 19 min and 100% B at 20 min. Separation was performed on a reversed phase ZORBAX Eclipse AAA (150 × 4.6 mm, 3.5 μm) column (Agilent Technologies) thermostated at 25 °C. The detection was performed by recording the absorption spectra between 240 nm and 400 nm. The measurement was made at 260 nm. For quantification, L-histidine monohydrochloride monohydrate (reagent grade, ≥98%, Sigma-Aldrich) was used as a standard compound and a calibration curve was built based on peak areas at 100, 50 and 25 μg/mL.

Extraction of total proteins and immunoblot analysis

Total protein extraction was performed for immunoblots as described in 89 unless otherwise indicated. Nitrocellulose and polyvinylidene difluoride (PVDF, in the case of CRY-DASH1, D1, D2 and PsaC) membranes, respectively, were used for immunoblots. Membranes were blocked with 5% (w/v) milk powder in Tris-buffered saline containing 0.1% (v/v) Tween-20 (TBS, pH 7.4). When using anti-rbcL (AS03 037, Agrisera), anti-CRY-DASH1,[31] anti-D1 (AS05 084, Agrisera), anti-D2 (AS06 146, Agrisera) and anti-PsaC (AS10 939, Agrisera) antibodies membranes were blocked overnight at 4 °C, for anti-CHLI1 (MBS7152864, Mybiosource) and anti-PAT2 (AS07 276, Agrisera) antibodies, membranes were blocked 2 h at room temperature. Membranes were incubated with the anti-rbcL in a dilution of 1: 15,000 and with anti-CRY-DASH1 in a dilution of 1:5,000 for 2 h at room temperature. With all other antibodies (with anti-CHLI1 in a dilution of 1:4,000, with anti-PAT2 in a dilution of 1:250, with anti-D1 and anti-D2 in a dilution of 1:25,000 and with anti-PsaC in a dilution of 1:5,000), membranes were incubated overnight at 4 °C and in case of anti-PAT2 two additional h at room temperature. For generation of immunoblots for Supplementary Figure 2, a new charge of the anti-CHLI1 antibody had to be ordered that required a dilution of 1:1,000. As secondary antibody, horseradish peroxidase-conjugated anti-rabbit IgGs (Sigma-Aldrich) with a dilution of 1:5,000 was used. Peroxidase activity was detected by a chemiluminescence assay as shown before.[4] As loading controls, nitrocellulose membranes were stained with Ponceau S and PVDF membranes were stained with Coomassie Brilliant Blue R 250 Protein quan-

tification was performed using IMAGEJ v.1.50b (National Institutes of Health).

PSI/PSII ratio

The ratio was estimated by performing quantitative immunoblot analysis using anti-PsaC and anti-D1/PsbA (see details under immunoblots above) from three replicates. Ratio calculation was done on a sample-by-sample basis according to https://www.agrisera.com/en/artiklar/psi-photosystem-i/index.html.[90]

Transcript analysis

The RNeasy Plant Mini Kit (Qiagen) was used to isolate total RNA from 15 mL of a photoautrophically grown *C. reinhardtii* culture of wild type strain SAG73.72 and *cry-dash1*$_{mut}$, respectively, with a concentration of 3–5 $\times$ 10^6 cells/mL harvested at LD4. To analyse the relative transcript abundance of the genes of interest by quantitative reverse transcription PCR (qRT-PCR), the Luna Universal One-Step RT-qPCR Kit (New England Biolabs) was used. Reactions containing 250 ng RNA in a volume of 20 μL were assayed in an AriaMx Real-Time PCR System (Agilent Technologies).

The *RACK1* (*Receptor of activated protein kinase C1*) gene was used as reference[4] along with the primers OMM2718 (5′-CTTCTCGCCCATGACCAC-3′) and OMM2719 (5′-CCCACCAGGTTGTTCTTCAG-3′). The following primers were used to amplify the target genes: *CHLI1* (OMM3018 5′-AGGTGTTCGGCATGGAGTAAGC-3′ and OMM3019 5′-GCCTTTCCGCAAATGCTCCAAC-3′), *CHLH1* (OMM3020 5′-ACGCCAAGAACTCCAAGGTGTG-3′ and OMM3021 5′- TGAGCGAGCCGATGA AGATGTT-3′), *CHLD1* (OMM3012 5′-ACATTGAGGCGTCCATGAAGGAG-3′ and OMM3013 5′-CGTCATCCAGCAGGTTGATCTC-3′), *CHLG1* (OMM3016 5′-TGGATTTGCGTGTCCACCATCG-3′ and OMM3017 5′-AAGTAGATCTGCGGCAGGATGAG-3′), *PAT2* (OMM3049 5′-TGGGCTTCTTTGAGCCCATTGC-3′ and OMM3050 5′-TAGCTCAA CGTGGCGGTCAATAC-3′), *PYK1* (OMM3051 5′-ACCGACTGCGTCATGCTTTC-3′ and OMM3052 5′-GGCAGATCTTGGTCATCACCTTC-3′) and *PFL1* (OMM3053 5′ TGCTGCTGGAGAAGAC AATGCG-3′ and OMM3054 5′-TCCAAGCGTCAAAGACGGCCTAAC-3′).

In vitro RNA-binding assay

The *in vitro* RNA binding assay was done according to a published protocol.[78] The *psbA* 5′-end (Supplementary Figure 6(A)) was synthetically produced by Thermo Fisher Scientific in the vector pWL9 (Supplementary Figure 6(B)). pWL9 was linearized with *Kpn*I and *in vitro* transcription was done with T7 RNA polymerase (MEGAshortscript T7 Transcription Kit, Thermo Fisher Scientific) following the instruction from the producer using Biotin-14-CTP (Thermo Fisher Scientific) as label according to 78. The molar ratio of CTP to biotinylated-14-CTP was 2:1. 500 μL of streptavidin-coated paramagnetic beads (Streptavidin MagneSphere Paramagnetic Particles, Promega) were washed four times with 500 μL of transcript interacting buffer (1 M NaCl, 5 mM Tris–HCl, pH 7.5, 0.5 mM EDTA, pH 8.0). Then, 20 μg biotinylated transcripts in 200 μL of transcript interacting buffer were incubated with the washed streptavidin-coated beads for 1 h at room temperature with slight agitation. The unbound transcripts were removed by ten washing steps in 500 μL of transcript interacting buffer and equilibrated eight times in 500 μL of washing buffer (80 mM NaCl, 10 mM Tris-HCl, pH 7.5, 1 mM EDTA, pH 8.0, 2 mM dithiothreitol, 5% [v/v] glycerol, 0.5% [v/v] Igepal CA-630, 25 μg/mL yeast RNA (Sigma-Aldrich), 1 $\times$ proteinase inhibitor cocktail (EDTA-free, Roche). One microgram purified His-tagged CRY-DASH1 protein (purified by Ni- and Heparin-affinity chromatographies and a 50 kDa size exclusion centrifuge filter) in 500 μL of incubating buffer (80 mM NaCl, 10 mM Tris-HCl, pH 7.5, 1 mM EDTA, pH 8.0, 2 mM dithiothreitol, 5% [v/v] glycerol, 1 $\times$ proteinase inhibitor cocktail (EDTA-free, Roche) was incubated with the equilibrated streptavidin-coated beads. After incubation at 4 °C with slight agitation for 2 h, the beads were washed five times with washing buffer containing yeast RNA (one time with 200 μL and four times with 500 μL) followed by six washing steps of 500 μL washing buffer without yeast RNA. Finally, bound proteins were eluted from the beads by incubation in 210 μL elution buffer (3 M NaCl, 10 mM Tris-HCl, pH 7.5, 1 mM EDTA, pH 8.0, 5% [v/v] glycerol) for 45 min at 4 °C with slight agitation.

Accession numbers

Cre gene identifier accession numbers according to Phytozome genome ID: 707 (*Chlamydomonas reinhardtii* CC-4532 v6.1):

CRE01.G007950_4532, CRE01.G015000_4532, CRE01.G015350_4532, CRE01.G016300_4532, CRE01.G032650_4532, CRE01.G042750_4532, CRE01.G044800_4532, CRE01.G050150_4532, CRE01.G054150_4532, CRE02.G078939_4532, CRE02.G085450_4532, CRE02.G093450_4532, CRE02.G097550_4532, CRE02.G107300_4532, CRE02.G141100_4532, CRE02.G142200_4532, CRE02.G142351_4532, CRE02.G143650_4532, CRE03.G144807_4532, CRE03.G145247_4532, CRE03.G146167_4532, CRE03.G177500_4532, CRE03.G189300_4532, CRE03.G197500_4532, CRE03.G203850_4532, CRE04.G226850_4532, CRE05.G240800_4532, CRE05.G241650_4532, CRE05.G242000_4532, CRE06.G257000_4532, CRE06.G261750_4532, CRE06.G262900_4532, CRE06.G270100_4532, CRE06.G273700_4532, CRE06.G274650_4532, CRE06.G278086_4532, CRE06.G278210_4532, CRE06.G285150_4532,

CRE06.G294750_4532, CRE06.G306300_4532, CRE06.G311850_4532, CRE06.G800656_4532, CRE07.G315700_4532, CRE07.G323600_4532, CRE07.G325500_4532, CRE07.G327400_4532, CRE07.G328200_4532, CRE07.G330250_4532, CRE07.G332300_4532, CRE07.G335200_4532, CRE07.G341850_4532, CRE07.G353450_4532, CRE08.G370650_4532, CRE08.G372000_4532, CRE08.G379200_4532, CRE08.G380201_4532, CRE09.G393173_4532, CRE09.G394850_4532, CRE09.G396650_4532, CRE09.G410250_4532, CRE09.G410650_4532, CRE09.G411200_4532, CRE10.G421700_4532, CRE10.G430150_4532, CRE10.G435300_4532, CRE10.G436350_4532, CRE10.G452350_4532, CRE10.G456750_4532, CRE10.G458550_4532, CRE11.G467535_4532, CRE11.G467767_4532, CRE11.G467778_4532, CRE11.G476750_4532, CRE11.G481500_4532, CRE12.G484200_4532, CRE12.G485150_4532, CRE12.G486100_4532, CRE12.G496700_4532, CRE12.G501050_4532, CRE12.G503550_4532, CRE12.G507558_4532, CRE12.G509650_4532, CRE12.G512600_4532, CRE12.G513750_4532, CRE12.G516450_4532, CRE12.G519900_4532, CRE12.G526800_4532, CRE12.G533550_4532, CRE12.G534250_4532, CRE12.G538700_4532, CRE12.G553700_4532, CRE12.G556250_4532, CRE12.G558450_4532, CRE12.G560950_4532, CRE12.G561000_4532, CRE13.G564050_4532, CRE13.G569350_4532, CRE13.G577100_4532, CRE13.G577850_4532, CRE13.G586050_4532, CRE13.G590500_4532, CRE13.G592200_4532, CRE13.G602350_4532, CRE13.G603176_4532, CRE14.G610501_4532, CRE14.G618050_4532, CRE14.G630859_4532, CRE15.G801860_4532, CRE16.G654500_4532, CRE16.G655050_4532, CRE16.G675550_4532, CRE16.G693500_4532, CRE16.G694400_4532, CRE16.G694850_4532, CRE17.G698450_4532, CRE17.G702150_4532, CRE17.G721500_4532, CRE17.G726750_4532, CRE17.G739752_4532, CRECp.G802277_4532, CRECp.G802283_4532, CRECp.G802300_4532, CRECp.G802303_4532, CRECp.G802321_4532, CRECp.G802331_4532.

DATA AVAILABILITY

Data will be made available on request.

DECLARATION OF COMPETING INTEREST

The authors declare that they have no known competing financial interests or personal relationships that could have appeared to influence the work reported in this paper.

Acknowledgements

We thank Sandra Künzel for assistance with cultures. M.M. received funding from the Deutsche Forschungsgemeinschaft by DFG grant Mi373/16-1 and within the frame of the DFG Cluster of Excellence EXC2051 Balance of the Microverse—Project-ID 390713860 T.V. was funded by the Carl-Zeiss foundation with a JSMC fellowship. The mass spectrometry unit was provided by EFRE (Europa für Thüringen, Europäische Fonds für Regionale Entwicklung) grant '2019 FGI 0025' to M.M.

Author contributions

M.M., A.R. and J.P. designed research; A.R., J. P., V.W., T.V., WS.L., W.L. and L.S. performed research. All authors analyzed data. A.R., J.P., V. W. and M.M. wrote the paper, with input from all co-authors.

Appendix A. Supplementary material

Supplementary material to this article can be found online at https://doi.org/10.1016/j.jmb.2023.168271.

Received 17 June 2023;
Accepted 6 September 2023;
Available online 10 September 2023

Keywords:
Chlamydomonas reinhardtii;
central carbon metabolism;
chlorophyll biosynthesis;
light signaling;
photoreceptor

† Current address: Wuhan Institute of Biomedical Sciences, School of Medicine, Jianghan University, 430056 Wuhan, China.

Abbreviations:
aCRY, Animal-like cryptochrome; ACS, Acetyl-CoA synthetase/ligase; AGC, Automatic gain control; AICAR-P, Aminoimidazole carboxamide ribonucleotide monophosphate; CHLD,I,H, Mg-chelatase; CHLG, Chlorophyll synthetase; CHLM, Mg-protoporphyrin IX methyltransferase; CP43, chlorophyll-binding protein of approximately 43 kDa; CPX, Coproporphyrinogen III oxidase; CRY, Cryptochrome; CRY-DASH1 also named DCRY1, *Drosophila, Arabidopsis, Synechocystis, Homo*-cryptochrome 1; ESI, Electrospray ionisation; FBA, Fructose-1,6-bisphosphate aldolase; FDR, False discovery rate; Fru-P, Fructose-phosphate; GAPC, Glyceraldehyde 3-phosphate dehydrogenase; GGPS, Geranylgeranyl pyrophosphate synthase; GND, 6-phosphogluconate dehydrogenase; GP, Glyceraldehyde-phosphate; GPD, Glycerol-3-phosphate dehydrogenase; GS, Glutamine synthase; HCD, Higher-energy collisional dissociation; HCF, High chlorophyll fluorescence; HIS1, Histidine biosynthesis, N-5-phosphoribosyl-ATP transferase; HIS7, Histidine biosynthesis, imidazole glycerol phosphate synthase; LC, Liquid chromatography; MEC, 2-C-methyl-D-erythritol 2,4-cyclodiphosphate

synthase; MS, Mass spectrometry; NSAF, Normalized spectral abundance factor; NTRC, NADPH-dependent thioredoxin reductase C; OPA, O-phthaldialdehyde; PAT, Phosphate acetyltransferase; pCRY, Plant cryptochrome; PDS, Phytoene desaturase; PFK, Phosphofructokinase; PFL, Pyruvate-formate lyase; PGA, Phosphoglycerate; PGM, Phosphoglucomutase; POR, Protochlorophyllide oxidoreductase; PRPP, Phosphoribosyl pyrophosphate; PSAG, Photosystem I reaction center subunit V; PSAH, Photosystem I reaction center subunit H; PSB33, PSII assembly protein; PVDF, Polyvinylidene fluoride; PYK, Pyruvate kinase; RACK1, Receptor of activated protein kinase C1; rbcL, Ribulose-1,5-bisphosphate carboxylase/oxygenase large subunit; Ru5P, Ribulose-5-phosphate; RuBP, Ribulose-1,5-bisphosphate; SpC, Spectral counts; TAL, Transaldolase; THF, Tetrahydrofuran

References

1. Chaves, I., Pokorny, R., Byrdin, M., Hoang, N., Ritz, T., Brettel, K., Essen, L.O., Van Der Horst, G.T.J., Batschauer, A., Ahmad, M., (2011). The cryptochromes: blue light photoreceptors in plants and animals. *Annu. Rev. Plant Biol.* **62**, 335–364. https://doi.org/10.1146/annurev-arplant-042110-103759.
2. Christie, J.M., Blackwood, L., Petersen, J., Sullivan, S., (2015). Plant flavoprotein photoreceptors. *Plant Cell Physiol.* **56**, 401–413. https://doi.org/10.1093/pcp/pcu196.
3. Deppisch, P., Helfrich-Förster, C., Senthilan, P.R., (2022). The gain and loss of cryptochrome/photolyase family members during evolution. *Genes (Basel)* **13** https://doi.org/10.3390/genes13091613.
4. Beel, B., Prager, K., Spexard, M., Sasso, S., Weiss, D., Müller, N., Heinnickel, M., Dewez, D., Ikoma, D., Grossman, A.R., Kottke, T., Mittag, M., (2012). A flavin binding cryptochrome photoreceptor responds to both blue and red light in *Chlamydomonas reinhardtii*. *Plant Cell* **24**, 2992–3008. https://doi.org/10.1105/tpc.112.098947.
5. Oldemeyer, S., Mittag, M., Kottke, T., (2019). Time-resolved infrared and visible spectroscopy on cryptochrome aCRY: basis for red light reception. *Biophys. J.* **117**, 490–499. https://doi.org/10.1016/j.bpj.2019.06.027.
6. Coesel, S., Mangogna, M., Ishikawa, T., Heijde, M., Rogato, A., Finazzi, G., Todo, T., Bowler, C., Falciatore, A., (2009). Diatom PtCPF1 is a new cryptochrome/photolyase family member with DNA repair and transcription regulation activity. *EMBO Rep.* **10**, 655–661. https://doi.org/10.1038/embor.2009.59.
7. Franz, S., Ignatz, E., Wenzel, S., Zielosko, H., Putu, E.P.G. N., Maestre-Reyna, M., Tsai, M.-D., Yamamoto, J., Mittag, M., Essen, L.-O., (2018). Structure of the bifunctional cryptochrome aCRY from *Chlamydomonas reinhardtii*. *Nucleic Acids Res.* **46**, 8010–8022. https://doi.org/10.1093/nar/gky621.
8. Ahmad, M., Cashmore, A.R., (1993). HY4 gene of *A. thaliana* encodes a protein with characteristics of a blue-light photoreceptor. *Nature* **366**, 162–166. https://doi.org/10.1038/366162a0.
9. Petersen, J., Rredhi, A., Szyttenholm, J., Mittag, M., (2022). Evolution of circadian clocks along the green lineage. *Plant Physiol.*. https://doi.org/10.1093/plphys/kiac141.
10. Patton, A.P., Hastings, M.H., (2023). The mammalian circadian time-keeping system. *J. Huntingtons. Dis.*, 1–14. https://doi.org/10.3233/JHD-230571.
11. Hammad, M., Albaqami, M., Pooam, M., Kernevez, E., Witczak, J., Ritz, T., Martino, C., Ahmad, M., (2020). Cryptochrome mediated magnetic sensitivity in: *Arabidopsis* occurs independently of light-induced electron transfer to the flavin. *Photochem. Photobiol. Sci.* **19**, 341–352. https://doi.org/10.1039/c9pp00469f.
12. Wiltschko, R., Nießner, C., Wiltschko, W., (2021). The magnetic compass of birds: the role of cryptochrome. *Front. Physiol.* **12** https://doi.org/10.3389/fphys.2021.667000.
13. Steele, J.H., (1974). 2. Marine Food Webs. *In: Struct. Mar. Ecosyst.*. Harvard University Press, pp. 9–28. https://doi.org/10.4159/harvard.9780674592513.c4.
14. McCutcheon, J., Lutz, S., Williamson, C., Cook, J.M., Tedstone, A.J., Vanderstraeten, A., Wilson, S.A., Stockdale, A., Bonneville, S., Anesio, A.M., Yallop, M.L., McQuaid, J.B., Tranter, M., Benning, L.G., (2021). Mineral phosphorus drives glacier algal blooms on the Greenland ice sheet. *Nature Commun.* **12** https://doi.org/10.1038/s41467-020-20627-w.
15. Field, C.B., Behrenfeld, M.J., Randerson, J.T., Falkowski, P., (1998). Primary production of the biosphere: integrating terrestrial and oceanic components. *Science (80-.)* **281**, 237–240. https://doi.org/10.1126/science.281.5374.237.
16. Petersen, J., Rredhi, A., Szyttenholm, J., Oldemeyer, S., Kottke, T., Mittag, M., (2021). The world of algae reveals a broad variety of cryptochrome properties and functions. *Front. Plant Sci.* **12** https://doi.org/10.3389/fpls.2021.766509.
17. Falciatore, A., Bailleul, B., Boulouis, A., Bujaldon, S., Cheminant-navarro, S., De Vitry, C., Eberhard, S., Jaubert, M., Kuras, R., Lafontaine, I., Landier, S., Selles, J., Vallon, O., Wostriko, K., (2022). Light-driven processes: key players of the functional biodiversity in microalgae. *Comptes Rendus. Biol.* **345** https://doi.org/10.5802/crbiol.80.
18. Ian K. Blaby, D.L., Blaby-Haas, C., Tourasse, N., Hom, E. F.Y., Munevver Aksoy, M.P., Grossman, A., Umen, J., Dutcher, S., Stephen King, D., Witman, G., Stanke, M., Harris, E.H., Goodstein, S.S., Grimwood, J., Schmutz, J., Olivier Vallon, M., Prochnik, S., (2014). The *Chlamydomonas* genome project: a decade on. *Trends Plant Sci.* **19**, 672–680. https://doi.org/10.1016/j.tplants.2014.05.008.
19. Craig, R.J., Gallaher, S.D., Shu, S., Salomé, P.A., Jenkins, J.W., Blaby-Haas, C.E., Purvine, S.O., O'Donnell, S., Barry, K., Grimwood, J., Strenkert, D., Kropat, J., Daum, C., Yoshinaga, Y., Goodstein, D.M., Vallon, O., Schmutz, J., Merchant, S.S., (2023). The *Chlamydomonas* genome project, version 6: reference assemblies for mating-type plus and minus strains reveal extensive structural mutation in the laboratory. *Plant Cell* **35**, 644–672. https://doi.org/10.1093/plcell/koac347.
20. Reisdorph, N.A., Small, G.D., (2004). The CPH1 gene of *Chlamydomonas reinhardtii* encodes two forms of cryptochrome whose levels are controlled by light-induced proteolysis. *Plant Physiol.* **134**, 1546–1554. https://doi.org/10.1104/pp.103.031930.
21. Müller, N., Wenzel, S., Zou, Y., Künzel, S., Sasso, S., Weiß, D., Prager, K., Grossman, A., Kottke, T., Mittag, M., (2017). A plant cryptochrome controls key features of the

Chlamydomonas circadian clock and its life cycle. *Plant Physiol.* **174**, 185–201. https://doi.org/10.1104/pp.17.00349.
22. Zou, Y., Wenzel, S., Müller, N., Prager, K., Jung, E.M., Kothe, E., Kottke, T., Mittag, M., (2017). An animal-like cryptochrome1 controls the *Chlamydomonas* sexual cycle. *Plant Physiol.* **174**, 1334–1347. https://doi.org/10.1104/pp.17.00493.
23. Brudler, R., Hitomi, K., Daiyasu, H., Toh, H., Kucho, K., Ishiura, M., Kanehisa, M., Roberts, V.A., Todo, T., Tainer, J.A., Getzoff, E.D., (2003). Identification of a new cryptochrome class. *Mol. Cell* **11**, 59–67. https://doi.org/10.1016/S1097-2765(03)00008-X.
24. Kottke, T., Oldemeyer, S., Wenzel, S., Zou, Y., Mittag, M., (2017). Cryptochrome photoreceptors in green algae: unexpected versatility of mechanisms and functions. *J. Plant Physiol.* **217**, 4–14. https://doi.org/10.1016/j.jplph.2017.05.021.
25. Kiontke, S., Göbel, T., Brych, A., Batschauer, A., (2020). DASH-type cryptochromes – solved and open questions. *Biol. Chem.* **401**, 1487–1493. https://doi.org/10.1515/hsz-2020-0182.
26. Selby, C.P., Sancar, A., (2006). A cryptochrome/photolyase class of enzymes with single-stranded DNA-specific photolyase activity. *Proc. Natl. Acad. Sci.* **103**, 17696–17700. https://doi.org/10.1073/pnas.0607993103.
27. Pokorny, R., Klar, T., Hennecke, U., Carell, T., Batschauer, A., Essen, L.-O., (2008). Recognition and repair of UV lesions in loop structures of duplex DNA by DASH-type cryptochrome. *Proc. Natl. Acad. Sci.* **105**, 21023–21027. https://doi.org/10.1073/pnas.0805830106.
28. Navarro, E., Niemann, N., Kock, D., Dadaeva, T., Gutiérrez, G., Engelsdorf, T., Kiontke, S., Corrochano, L. M., Batschauer, A., Garre, V., (2020). The DASH-type cryptochrome from the fungus *Mucor circinelloides* is a canonical CPD-photolyase. *Curr. Biol.* **30**, 4483–4490.e4. https://doi.org/10.1016/j.cub.2020.08.051.
29. Castrillo, M., García-Martínez, J., Avalos, J., (2013). Light-Dependent functions of the *Fusarium fujikuroi* CryD DASH cryptochrome in development and secondary metabolism. *Appl. Environ. Microbiol.* **79**, 2777–2788. https://doi.org/10.1128/AEM.03110-12.
[30]. Yang, X., Li, L., Wang, X., Yao, J., Duan, D., (2020). Non-coding RNAs participate in the regulation of CRY-DASH in the growth and early development of *Saccharina japonica* (Laminariales, Phaeophyceae). *Int. J. Mol. Sci.* **21**, 309. https://doi.org/10.3390/ijms21010309.
[31]. Rredhi, A., Petersen, J., Schubert, M., Li, W., Oldemeyer, S., Li, W., Westermann, M., Wagner, V., Kottke, T., Mittag, M., (2021). DASH cryptochrome 1, a UV-A receptor, balances the photosynthetic machinery of *Chlamydomonas reinhardtii*. *New Phytol.* **232**, 610–624. https://doi.org/10.1111/nph.17603.
32. Mason, C.B., Bricker, T.M., Moroney, J.V., (2006). A rapid method for chloroplast isolation from the green alga *Chlamydomonas reinhardtii*. *Nature Protoc.* **1**, 2227–2230. https://doi.org/10.1038/nprot.2006.348.
33. Yang, M., Jiang, J.P., Xie, X., Chu, Y.D., Fan, Y., Cao, X. P., Xue, S., Chi, Z.Y., (2017). Chloroplasts isolation from *Chlamydomonas reinhardtii* under nitrogen stress, Front. *Plant Sci.* **8**, 1–12. https://doi.org/10.3389/fpls.2017.01503.
34. Schellenberger Costa, B., Jungandreas, A., Jakob, T., Weisheit, W., Mittag, M., Wilhelm, C., (2013). Blue light is essential for high light acclimation and photoprotection in the diatom *Phaeodactylum tricornutum*. *J. Exp. Bot.* **64**, 483–493. https://doi.org/10.1093/jxb/ers340.
35. Rozanova, S., Barkovits, K., Nikolov, M., Schmidt, C., Urlaub, H., Marcus, K., (2021). Quantitative mass spectrometry-based proteomics: an overview. *In: Methods Mol. Biol.* Humana Press Inc., pp. 85–116. https://doi.org/10.1007/978-1-0716-1024-4_8.
36. Johnson, X., Alric, J., (2013). Central carbon metabolism and electron transport in *Chlamydomonas reinhardtii*: metabolic constraints for carbon partitioning between oil and starch. *Eukaryot. Cell* **12**, 776–793. https://doi.org/10.1128/EC.00318-12.
37. Yang, W., Catalanotti, C., D'adamo, S., Wittkopp, T.M., Ingram-Smith, C.J., Mackinder, L., Miller, T.E., Heuberger, A.L., Peers, G., Smith, K.S., Jonikas, M.C., Grossman, A. R., Posewitz, M.C., (2014). Alternative acetate production pathways in *Chlamydomonas reinhardtii* during dark anoxia and the dominant role of chloroplasts in fermentative acetate production. *Plant Cell* **26**, 4499–4518. https://doi.org/10.1105/tpc.114.129965.
38. Catalanotti, C., Dubini, A., Subramanian, V., Yang, W., Magneschi, L., Mus, F., Seibert, M., Posewitz, M.C., Grossman, A.R., (2012). Altered fermentative metabolism in *Chlamydomonas reinhardtii* mutants lacking pyruvate formate lyase and both pyruvate formate lyase and alcohol dehydrogenase. *Plant Cell* **24**, 692–707. https://doi.org/10.1105/tpc.111.093146.
39. Muralla, R., Sweeney, C., Stepansky, A., Leustek, T., Meinke, D., (2007). Genetic dissection of histidine biosynthesis in *Arabidopsis*. *Plant Physiol.* **144**, 890–903. https://doi.org/10.1104/pp.107.096511.
40. Reyes-Prieto, A., Moustafa, A., (2012). Plastid-localized amino acid biosynthetic pathways of Plantae are predominantly composed of non-cyanobacterial enzymes. *Sci. Rep.* **2**, 1–12. https://doi.org/10.1038/srep00955.
41. Vallon, O., Spalding, M.H., (2009). Amino acid metabolism. *Chlamydomonas Sourceb*, **3-Vol Set** Elsevier Inc., pp. 115–158. https://doi.org/10.1016/B978-0-12-370873-1.00012-5.
42. Milito, A., Castellano, I., Burn, R., Seebeck, F.P., Brunet, C., Palumbo, A., (2020). First evidence of ovothiol biosynthesis in marine diatoms. *Free Radic. Biol. Med.* **152**, 680–688. https://doi.org/10.1016/j.freeradbiomed.2020.01.010.
43. Sakato-Antoku, M., King, S.M., (2022). Developmental changes in ciliary composition during gametogenesis in *Chlamydomonas*. *Mol. Biol. Cell* **33**, 1–10. https://doi.org/10.1091/mbc.E22-02-0033.
44. Greiner, A., Kelterborn, S., Evers, H., Kreimer, G., Sizova, I., Hegemann, P., (2017). Targeting of photoreceptor genes in *Chlamydomonas reinhardtii* via zinc-finger nucleases and CRISPR/Cas9. *Plant Cell* **29**, 2498–2518. https://doi.org/10.1105/tpc.17.00659.
45. Tian, Y., Gao, S., Heyde, E.L., Hallmann, A., Nagel, G., (2018). Two-component cyclase opsins of green algae are ATP-dependent and light-inhibited guanylyl cyclases. *BMC Biol.* **16**, 1–18. https://doi.org/10.1186/s12915-018-0613-5.
46. Ort, D.R., Zhu, X., Melis, A., (2011). Optimizing antenna size to maximize photosynthetic efficiency. *Plant Physiol.* **155**, 79–85. https://doi.org/10.1104/pp.110.165886.
47. Beale, S.I., (2009). Biosynthesis of chlorophylls and hemes. *Chlamydomonas Sourceb* **3-Vol Set. 2**, 731–798. https://doi.org/10.1016/B978-0-12-370873-1.00028-9.

48. Richter, A.S., Pérez-Ruiz, J.M., Cejudo, F.J., Grimm, B., (2018). Redox-control of chlorophyll biosynthesis mainly depends on thioredoxins. *FEBS Lett.* **592**, 3111–3115. https://doi.org/10.1002/1873-3468.13216.
49. Fleischer, E.B., Miller, C.K., Webb, L.E., (1964). Crystal and molecular structures of some metal tetraphenylporphines. *J. Am. Chem. Soc.* **86**, 2342–2347. https://doi.org/10.1021/ja01066a009.
50. Jensen, P.E., Willows, R.D., Petersen, B.L., Vothknecht, U. C., Stummann, B.M., Kannangara, C.G., Von Wettstein, D., Henningsen, K.W., (1996). Structural genes for Mg-chelatase subunits in barley: Xantha-f, -g and -h. *Mol. Gen. Genet.* **250**, 383–394. https://doi.org/10.1007/s004380050090.
51. Ikegami, A., Yoshimura, N., Motohashi, K., Takahashi, S., Romano, P.G.N., Hisabori, T., Takamiya, K.I., Masuda, T., (2007). The CHLI1 subunit of *Arabidopsis thaliana* magnesium chelatase is a target protein of the chloroplast thioredoxin. *J. Biol. Chem.* **282**, 19282–19291. https://doi.org/10.1074/jbc.M703324200.
52. Oliver, R.P., Griffiths, W.T., (1981). Covalent labelling of the NADPH: protochlorophyllide oxidoreductase from etioplast membranes with [3H]N-phenylmaleimide. *Biochem. J* **195**, 93–101. https://doi.org/10.1042/bj1950093.
53. Schoch, S., (1978). The esterification of chlorophyllide a in greening bean leaves. *Zeitschrift Fur Naturforsch. - Sect. C J. Biosci.* **33**, 712–714. https://doi.org/10.1515/znc-1978-9-1018.
54. Proctor, M.S., Chidgey, J.W., Shukla, M.K., Jackson, P.J., Sobotka, R., Hunter, C.N., Hitchcock, A., (2018). Plant and algal chlorophyll synthases function in *Synechocystis* and interact with the YidC/Alb3 membrane insertase. *FEBS Lett.* **592**, 3062–3073. https://doi.org/10.1002/1873-3468.13222.
55. Carrillo, L.R., Froehlich, J.E., Cruz, J.A., Savage, L.J., Kramer, D.M., (2016). Multi-level regulation of the chloroplast ATP synthase: the chloroplast NADPH thioredoxin reductase C (NTRC) is required for redox modulation specifically under low irradiance. *Plant J.* **87**, 654–663. https://doi.org/10.1111/tpj.13226.
56. Pérez-Ruiz, J.M., Spínola, M.C., Kirchsteiger, K., Moreno, J., Sahrawy, M., Cejudo, F.J., (2006). Rice NTRC is a high-efficiency redox system for chloroplast protection against oxidative damage. *Plant Cell* **18**, 2356–2368. https://doi.org/10.1105/tpc.106.041541.
57. Carrera-Pacheco, S.E., Hankamer, B., Oey, M., (2023). Environmental and nuclear influences on microalgal chloroplast gene expression. *Trends Plant Sci.*, 1–13. https://doi.org/10.1016/j.tplants.2023.03.013.
58. M. Lohr, Carotenoids, *Chlamydomonas* Sourceb. 2-Vol Set. 2 (2009) 799–817. https://doi.org/10.1016/B978-0-12-370873-1.00028-9.
59. Varotto, C., Maiwald, D., Pesaresi, P., Jahns, P., Salamini, F., Leister, D., (2002). The metal ion transporter IRT1 is necessary for iron homeostasis and efficient photosynthesis in *Arabidopsis thaliana*. *Plant J.* **31**, 589–599. https://doi.org/10.1046/j.1365-313X.2002.01381.x.
60. Minagawa, J., Tokutsu, R., (2015). Dynamic regulation of photosynthesis in *Chlamydomonas reinhardtii*. *Plant J.* **82**, 413–428. https://doi.org/10.1111/tpj.12805.
61. Ozawa, S.I., Bald, T., Onishi, T., Xue, H., Matsumura, T., Kubo, R., Takahashi, H., Hippler, M., Takahashi, Y., (2018). Configuration of ten light-harvesting chlorophyll a/b complex i subunits in *Chlamydomonas reinhardtii* photosystem I. *Plant Physiol.* **178**, 583–595. https://doi.org/10.1104/pp.18.00749.
62. Nilsson, A.K., Pěnčík, A., Johansson, O.N., Bånkestad, D., Fristedt, R., Suorsa, M., Trotta, A., Novák, O., Mamedov, F., Aro, E.M., Burmeister, B.L., (2020). PSB33 protein sustains photosystem II in plant chloroplasts under UV-A light. *J. Exp. Bot.* **71**, 7210–7223. https://doi.org/10.1093/jxb/eraa427.
63. Meurer, J., Plücken, H., Kowallik, K.V., Westhoff, P., (1998). A nuclear-encoded protein of prokaryotic origin is essential for the stability of photosystem II in *Arabidopsis thaliana*. *EMBO J.* **17**, 5286–5297. https://doi.org/10.1093/emboj/17.18.5286.
64. Komenda, J., Nickelsen, J., Tichý, M., Prášil, O., Eichacker, L.A., Nixon, P.J., (2008). The cyanobacterial homologue of HCF136/YCF48 is a component of an early photosystem II assembly complex and is important for both the efficient assembly and repair of photosystem II in *Synechocystis* sp. PCC 6803. *J. Biol. Chem.* **283**, 22390–22399. https://doi.org/10.1074/jbc.M801917200.
65. Plücken, H., Müller, B., Grohmann, D., Westhoff, P., Eichacker, L.A., (2002). The HCF136 protein is essential for assembly of the photosystem II reaction center in *Arabidopsis thaliana*. *FEBS Lett.* **532**, 85–90. https://doi.org/10.1016/S0014-5793(02)03634-7.
66. Schottkowski, M., Peters, M., Zhan, Y., Rifai, O., Zhang, Y., Zerges, W., (2012). Biogenic membranes of the chloroplast in *Chlamydomonas reinhardtii*. *PNAS* **109**, 19286–19291. https://doi.org/10.1073/pnas.1209860109.
[67]. Lee, J.W., Lee, S.H., Han, J.W., Kim, G.H., (2020). Early light-inducible protein (ELIP) can enhance resistance to cold-induced photooxidative stress in *Chlamydomonas reinhardtii*. *Front. Physiol.* **11**, 1–15. https://doi.org/10.3389/fphys.2020.01083.
68. Li, X., Bin Wang, H., Jin, H.L., (2020). Light signaling-dependent regulation of PSII biogenesis and functional maintenance. *Plant Physiol.* **183**, 1855–1868. https://doi.org/10.1104/pp.20.00200.
69. Chotewutmontri, P., Barkan, A., (2020). Light-induced *psbA* translation in plants is triggered by photosystem II damage via an assembly-linked autoregulatory circuit. *Proc. Natl. Acad. Sci.* **117**, 21775–21784. https://doi.org/10.1073/pnas.2007833117.
70. Wang, F., Dischinger, K., Westrich, L.D., Meindl, I., Egidi, F., Trösch, R., Sommer, F., Johnson, X., Schroda, M., Nickelsen, J., Willmund, F., Vallon, O., Bohne, A.-V., (2023). One-helix protein 2 is not required for the synthesis of photosystem II subunit D1 in *Chlamydomonas*. *Plant Physiol.* **191**, 1612–1633. https://doi.org/10.1093/plphys/kiad015.
71. Trebitsh, T., Levitan, A., Sofer, A., Danon, A., (2000). Translation of chloroplast psbA mRNA is modulated in the light by counteracting oxidizing and reducing activities. *Mol. Cell Biol.* **20**, 1116–1123. https://doi.org/10.1128/mcb.20.4.1116-1123.2000.
72. Im, C.S., Eberhard, S., Huang, K., Beck, C.F., Grossman, A.R., (2006). Phototropin involvement in the expression of genes encoding chlorophyll and carotenoid biosynthesis enzymes and LHC apoproteins in *Chlamydomonas reinhardtii*. *Plant J.* **48**, 1–16. https://doi.org/10.1111/j.1365-313X.2006.02852.x.
73. Rea, G., Antonacci, A., Lambreva, M.D., Mattoo, A.K., (2018). Features of cues and processes during chloroplast-

mediated retrograde signaling in the alga *Chlamydomonas*. *Plant Sci.* **272**, 193–206. https://doi.org/10.1016/j.plantsci.2018.04.020.
74. Chowdhury, M.N., Jin, H., (2022). The RGG motif proteins: Interactions, functions, and regulations. *Wiley Interdiscip. Rev. RNA* **14**, 1–23. https://doi.org/10.1002/wrna.1748.
75. Thandapani, P., O'Connor, T.R., Bailey, T.L., Richard, S., (2013). Defining the RGG/RG motif. *Mol. Cell* **50**, 613–623. https://doi.org/10.1016/j.molcel.2013.05.021.
76. Trebitsh, T., Danon, A., (2001). Translation of chloroplast *psbA* mRNA is regulated by signals initiated by both photosystems II and I. *PNAS* **98**, 12289–12294. https://doi.org/10.1073/pnas.211440698.
77. Mulo, P., Sakurai, I., Aro, E.M., (1817). Strategies for *psbA* gene expression in cyanobacteria, green algae and higher plants: from transcription to PSII repair. *Biochim. Biophys. Acta – Bioenerg.* **2012**, 247–257. https://doi.org/10.1016/j.bbabio.2011.04.011.
78. Zhao, B., Schneid, C., Iliev, D., Schmidt, E.-M., Wagner, V., Wollnik, F., Mittag, M., (2004). The circadian RNA-binding protein CHLAMY 1 represents a novel type heteromer of RNA recognition motif and lysine homology domain-containing subunits. *Eukaryot. Cell* **3**, 815–825. https://doi.org/10.1128/EC.3.3.815-825.2004.
79. Milojevic, T., Sonnleitner, E., Romeo, A., Djinovic-Carugo, K., Bläsi, U., (2013). False positive RNA binding activities after Ni-affinity purification from *Escherichia coli*. *RNA Biol.* **10**, 1066–1069. https://doi.org/10.4161/rna.25195.
80. Huang, K., Beck, C.F., (2003). Phototropin is the blue-light receptor that controls multiple steps in the sexual life cycle of the green alga *Chlamydomonas reinhardtii*. *PNAS* **100**, 6269–6274. https://doi.org/10.1073/pnas.0931459100.
81. Trippens, J., Greiner, A., Schellwat, J., Neukam, M., Rottmann, T., Lu, Y., Kateriya, S., Hegemann, P., Kreimer, G., (2012). Phototropin influence on eyespot development and regulation of phototactic behavior in *Chlamydomonas reinhardtii*. *Plant Cell* **24**, 4687–4702. https://doi.org/10.1105/tpc.112.103523.
82. Petroutsos, D., Tokutsu, R., Maruyama, S., Flori, S., Greiner, A., Magneschi, L., Cusant, L., Kottke, T., Mittag, M., Hegemann, P., Finazzi, G., Minagawa, J., (2016). A blue-light photoreceptor mediates the feedback regulation of photosynthesis. *Nature* **537**, 563–566. https://doi.org/10.1038/nature19358.
83. Arend, M., Yuan, Y., Ruiz-Sola, M.Á., Omranian, N., Nikoloski, Z., Petroutsos, D., (2022). Widening the landscape of transcriptional regulation of algal photoprotection. *Nature Commun.*. https://doi.org/10.1038/s41467-023-38183-4 2022.02.25.482034.
84. Levine, R.T., Ebersold, W.T., (1958). The relation of calcium and magnesium to crossing over in *Chlamydomonas reinhardtii*. *Zeitschr. f. Vererbungslehre* **89**, 631–635. https://doi.org/10.1007/BF00888552.
85. Harris, E.H., (1989). A comprehensive guide to biology and laboratory use. Academic Press. http://www.ncbi.nlm.nih.gov/pubmed/11337403.
86. Boesger, J., Wagner, V., Weisheit, W., Mittag, M., (2009). Analysis of flagellar phosphoproteins from *Chlamydomonas reinhardtii*. *Eukaryot. Cell* **8**, 922–932. https://doi.org/10.1128/EC.00067-09.
87. Link, A.J., Eng, J., Schieltz, D.M., Carmack, E., Mize, G.J., Morris, D.R., Garvik, B.M., Yates, J.R., (1999). Direct analysis of protein complexes using mass spectrometry. *Nature Biotechnol.* **17**, 676–682. https://doi.org/10.1038/10890.
88. Betancort Rodríguez, J.R., García Reina, G., Santana Rodríguez, J.J., (1997). Determination of free amino acids in microalgae by high-performance liquid chromatography using pre-column fluorescence derivatization. *Biomed. Chromatogr.* **11**, 335–336. https://doi.org/10.1002/(SICI)1099-0801(199711)11:6<335::AID-BMC684>3.3.CO;2-K.
89. Schulze, T., Schreiber, S., Iliev, D., Boesger, J., Trippens, J., Kreimer, G., Mittag, M., (2013). The heme-binding protein SOUL3 of *Chlamydomonas reinhardtii* influences size and position of the eyespot. *Mol. Plant* **6**, 931–944. https://doi.org/10.1093/mp/sss137.
90. Cecchin, M., Paloschi, M., Busnardo, G., Cazzaniga, S., Cuine, S., Li-Beisson, Y., Wobbe, L., Ballottari, M., (2021). CO_2 supply modulates lipid remodelling, photosynthetic and respiratory activities in *Chlorella* species. *Plant Cell Environ.* **44**, 2987–3001. https://doi.org/10.1111/pce.14074.
91. Kobayashi, K., Masuda, T., (2016). Transcriptional regulation of tetrapyrrole biosynthesis in *Arabidopsis thaliana*. *Front Plant Sci.* **7**, 1–17. https://doi.org/10.3389/fpls.2016.01811.